ISSN 0169-6548

Communications on hydraulic and geotechnical engineering

Application of sediment transport formulae to sand-dike breach erosion

1995

Paul J. Visser

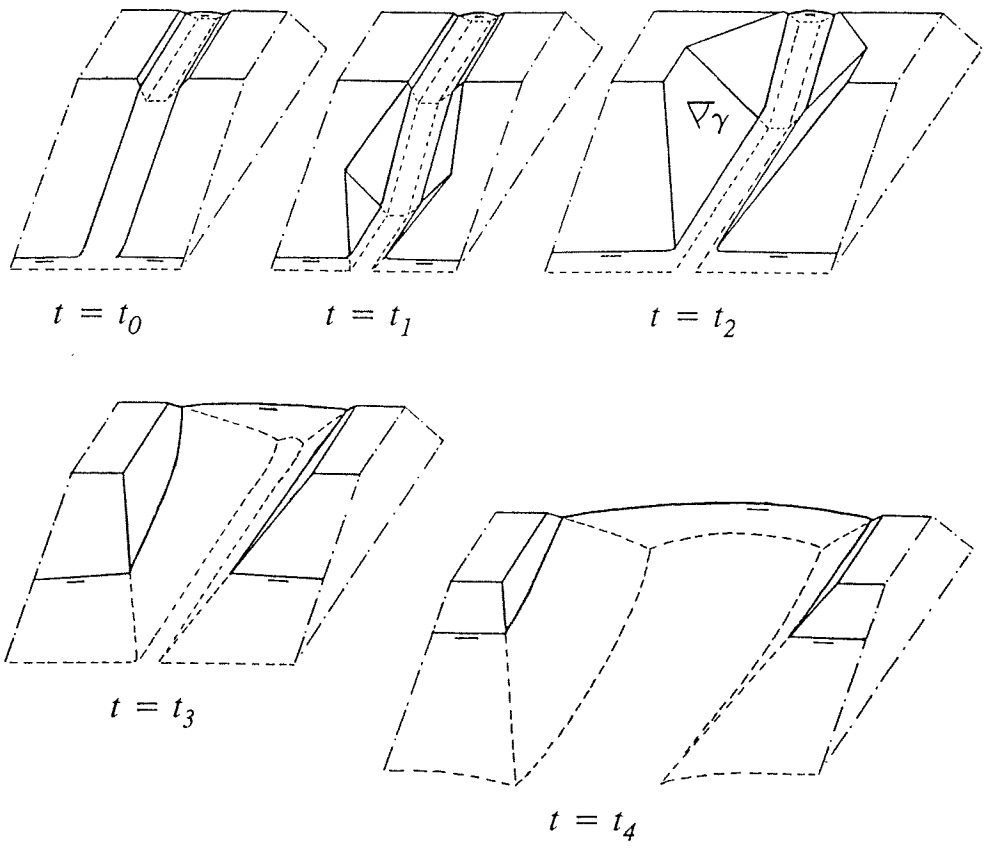

TU Delft
Delft University of Technology

Faculty of Civil Engineering

APPLICATION OF SEDIMENT TRANSPORT FORMULAE TO SAND-DIKE BREACH EROSION

Paul J. Visser

Communications on Hydraulic and Geotechnical Engineering
Report no. 94-7
Hydraulic and Geotechnical Engineering Division
Faculty of Civil Engineering
Delft University of Technology
1995

Contents

Contents (continuation)

Summary

The Technical Advisory Committee on Water Defences in the Netherlands has decided to develop a mathematical model for breach erosion in dunes and dikes, with which it will be possible to predict the growth of the breach and the discharge rate through the breach in case of a dike-burst. An essential part of such a mathematical model is the description of the entrainment of the sediment (sand or clay) and its transport through the breach. The process of breach erosion, especially in the first phases, is characterized by relatively steep slopes and large flow velocities. None of the existing sediment transport formulae has been derived and tested for these circumstances.

This report presents the results of an investigation into the applicability of sediment transport formulae to sand-dike breach erosion. In view of the steep slopes and the large flow velocities, the following sediment transport conceptions have been included in the study:

- formulae for sand-water mixture flows: Wilson (1966), Wilson (1987), Mastbergen and Winterwerp (1987);
- formulae for sediment transport in flows on relatively steep slopes: Mizuyama (1977), Smart and Jaeggi (1983), Bathurst et al. (1987), Takahashi (1987), Rickenmann (1991);
- formulae for river regimes which have been tested for (relatively) large flow velocities (large shear stress velocities): Engelund and Hansen (1967), Van Rijn (1984a, 1984c);
- energetics-based sediment transport conceptions: Bagnold (1963, 1966), Yang (1979), Bagnold-Bailard, see Bailard (1981), Bagnold-Visser, see Visser (1988), these last two formulae are modifications of the original conception of Bagnold (1963, 1966);
- formulae for debris flows: Takahashi (1978, 1980, 1987, 1991).

These sediment transport formulae, combined with Galappatti's model (1983) for the pick-up of sediment, are compared with the data of two laboratory experiments (Schelde Flume experiments, see Steetzel and Visser, 1992a, 1992b) and the data of a field experiment (Zwin'89 experiment, see Visser et al., 1990). Experimental sediment transport rates have been determined as volumes of sand eroded over a certain period of time. All tests concern super-critical flow (Froude number $Fr > 1$, i.e. here $2.8 \leq Fr \leq 4.1$), large values for Shields' mobility parameter ($10 < \theta < 100$) and high concentrations (depth-averaged values rising up to about 0.25 by volume).

Most of the tested sediment transport formulae predict sand transport rates being much larger than the observed quantities. Only the Bagnold-Visser formula, see Visser (1988), predicts sand transport rates within a factor two of the experimental values. With the formulation of Van Rijn (1984a, 1984c) this is possible within about a factor three. All other formulae give larger deviations from the experimental data.

These conclusions hold for the three initial phases of the process of breach erosion, when the flow is supercritical, and confirm the good results obtained up to now with the Bagnold-Visser formula, see Visser (1988, 1994). Once more it should be emphasized that this formula has not been derived for a situation where the rate of sand entrainment is so large as in the first three phases of the breach erosion process (this applies to both the energetics-based method and the semi-empirical determination of the efficiency factor). The relatively large entrainment of sediment causes a relatively large increase of both the flow rate and the sediment concentration of the sand-water mixture along the inner slope (so that the effect of 'hindered entrainment' is possibly not negligible). Further study is necessary to establish the effects of the large rate of sediment entrainment on the breach erosion process. For the time being it is recommended to apply the formula of Bagnold-Visser in a mathematical breach growth model for the description of the first phases (i.e. as long as the flow is supercritical) of the breach erosion process.

The present study does not recommend a formula for the important later phases of breach growth (when the flows becomes subcritical), in which most of the breach erosion takes place and in which also the dimensions of the ultimate breach are determined. Probably the data of the recent Zwin'94 field experiment (see Visser et al, 1995) will allow such a recommendation in the near future. For the present the conclusion of Voogt et al. (1991) is still valid, i.e. that the formulae of Engelund and Hansen (1967) and in particular Van Rijn (1984a, 1984c) can also be applied for relatively large current velocities in subcritical flow.

1 Introduction

The Technical Advisory Committee on Water Defences (TAW) in the Netherlands has decided (in 1991) to develop a probabilistic design method for dikes and dunes (hereafter both denominated as dikes). This method involves a procedure for the design and control of dikes based on a widely-accepted risk-norm (risk of inundation) instead of a chance-norm (chance of exceeding a certain water level) as in the present approach. A risk-norm means that the product of the probability of inundation and the consequences of flooding (deaths, loss of property and revenues, repair costs, etc.) is evaluated, see Kraak et al. (1994). To be able to determine the consequences of an inundation, it is necessary to predict the rate of polder flooding, which is above all governed by the flow rate through the breach in the dike. It is therefore of importance to have a mathematical model for breach erosion with which it is possible to predict the breach growth and the discharge rate through the breach as function of the parameters involved. These parameters are:

- geometry of the cross-section of the dike (height, width, angles of the slopes);
- structure of the dike (dike material, revetments, foundation);
- area of the polder;
- hydraulic conditions (water level against the dike, wave conditions).

An essential part of a mathematical model for breach erosion in a dike is the description for the pick-up and transport of the sediment (sand or clay). The flow velocities in breaches can become very large, for instance for a 10 m high dike about 7 m/s. There is no sediment transport formula that has been derived and tested for such large flow velocities (data of experiments on sand transport in flow velocities larger than about 3 m/s are not available, see Voogt et al., 1991, and Sieben, 1993). An additional complication is that less is known about the erosion of clay; most of the poor knowledge of erosion of cohesive sediment applies to the erosion of muddy bottoms (non-consolidated sediment).

The development of a first version of a breach growth model and its verification against laboratory experiments and a field experiment has been set out in Visser (1988, see also Visser et al., 1986) and Visser (1994). This model version describes the first phases (phases I, II, III, see chapter 2) of the breach erosion process. The comparisons with both laboratory tests and the Zwin'89 field experiment in the Zwin Channel (a tidal inlet at the Netherlands-Belgium border) show good agreement.

A modified Bagnold's (1963, 1966) energetics-based sediment transport formulation (here termed the Bagnold-Visser formula) has been implemented in this model combined with Galappatti's (1983, see also Galappatti and Vreugdenhil, 1985) description for sediment entrainment (see Visser, 1988). The choice for an energetics-based sediment transport conception has been dictated by the very large flow velocities, in order to avoid an enormous

overestimation of the entrainment and transport of sediment. However, in spite of the good results obtained so far with the Bagnold-Visser sand transport formulation, the question arises whether this formula is the best of all available formulae.

To answer this question the present investigation into the applicability of available sediment transport formulae for sand-dike breach erosion has been made. In view of the steep slopes and the large flow velocities, the following sediment transport conceptions have been included in the study:

1. Formulae for sand-water mixture flows: Wilson (1966), Wilson (1987), Mastbergen and Winterwerp (1987), see also Winterwerp et al. (1992).
2. Formulae for sediment transport in flows on relatively steep slopes: Mizuyama (1977), Smart and Jaeggi (1983), Bathurst et al. (1987), Takahashi (1987), Rickenmann (1991), see also the reviews of Jaeggi and Rickenmann (1987) and Takahashi (1987).
3. Formulae for river regimes which have been tested for (relatively) large flow velocities (large shear stress velocities): Engelund and Hansen (1967), Van Rijn (1984a, 1984c), see Voogt et al. (1991).
4. Energetics-based sediment transport conceptions: Bagnold (1963, 1966), Yang (1979), Bagnold-Bailard, see Bailard (1981), Bagnold-Visser, see Visser (1988), these last two formulae are modifications of the original conception of Bagnold (1963, 1966).
5. Formulae for debris flows: Takahashi (1978, 1980, 1987, 1991).

Chapter 2 contains a brief description of the breach erosion process. The sediment transport formulations under consideration are summarized in chapter 3, including the validity ranges (if known) and some background information. The sediment transport formulae are compared with the data of two laboratory experiments (Schelde Flume experiments, see Steetzel and Visser, 1992a, 1992b) and to the data of the Zwin'89 experiment (see Visser et al., 1990). Experimental sand transport rates have been determined by estimating the volumes of eroded bed material per time period from the observed bed profile developments.

The experimental data involve the first three phases of the breach erosion process (see chapter 2). So also the present investigation has been restricted to these first phases of the breach erosion process. The conclusions and recommendations are described in chapter 5.

2 Breach erosion process

Fig. 2.1 schematically shows the process of breach growth in a sand-dike. It is assumed that the breach erosion starts (at $t = t_0$) with the flow of water through a small initial breach at the crest and in the inner slope of the dike. The following phases can be distinguished in the breach erosion process (Visser, 1994):

I. Steepening of the inclination angle β of the (channel in the inner) slope from an initial value β_0 at $t = t_0$ up to a critical value β_1 at $t = t_1$ (see Fig. 2.1).

II. Continuation of the erosion of the inner slope, yielding a decrease of the width of the crest of the dike in the breach for $t_1 < t \leq t_2$; the slope angle of the inner slope remains (in this line of thought) at its critical value β_1.

III. Lowering of the top of the dike in the breach, with constant angle of the side slopes, resulting in an increase of the breach width for $t_2 < t < t_3$.

IV. After the complete wash-out of the dike in the breach, continuation of the breach growth in both vertical (scour hole) and horizontal direction for $t_3 \leq t < t_4$. At t_4 the flow through the breach is critical, i.e. changes from supercritical ($Fr > 1$ for $t < t_4$) to subcritical ($Fr < 1$ for $t > t_4$). It is clear that for very small polders the transition from supercritical flow into subcritical can take place for $t < t_4$.

V. Continuation of the increase of the breach width for $t_4 \leq t < t_5$. At t_5 the flow velocities in the breach become so small (incipient motion) that the breach erosion stops.

The flow on the inner slope for $t_0 < t < t_3$ and in the breach for $t_3 \leq t < t_4$ is supercritical, which means that, for realistic values of the head over the breach and the slope angle, the flow velocities can become very large. The slope angle β (see Fig. 2.2) is defined here as the inclination of the inner slope (or scour hole) in the flow direction with respect to a horizontal line. The inclination angle of the side slopes of the breach is here termed the side slope angle (γ), see Fig. 2.1.

The slope and side slope angles in the breach can become very large in the different phases of the breaching process. In the Schelde Flume experiments values for β larger than 45° were observed, see Figures 4.1 and 4.2. In both laboratory experiments (see Visser, 1988) and the Zwin'89 field experiment (see Visser et al., 1990) it was observed that the side slope angle temporarily can become very large (up to about 90° before the side slopes slide down).

The slope angle β plays an active role in the first three phases of the very dynamic breaching process. The role of the side slope angle in this process is more passive as the above tests indicate. Visser (1988) demonstrated theoretically that in the phases I, II and III the breach width increases linearly with the breach depth. Then, the side slope angle only influences the magnitude of the coupling factor between breach width and breach depth. After

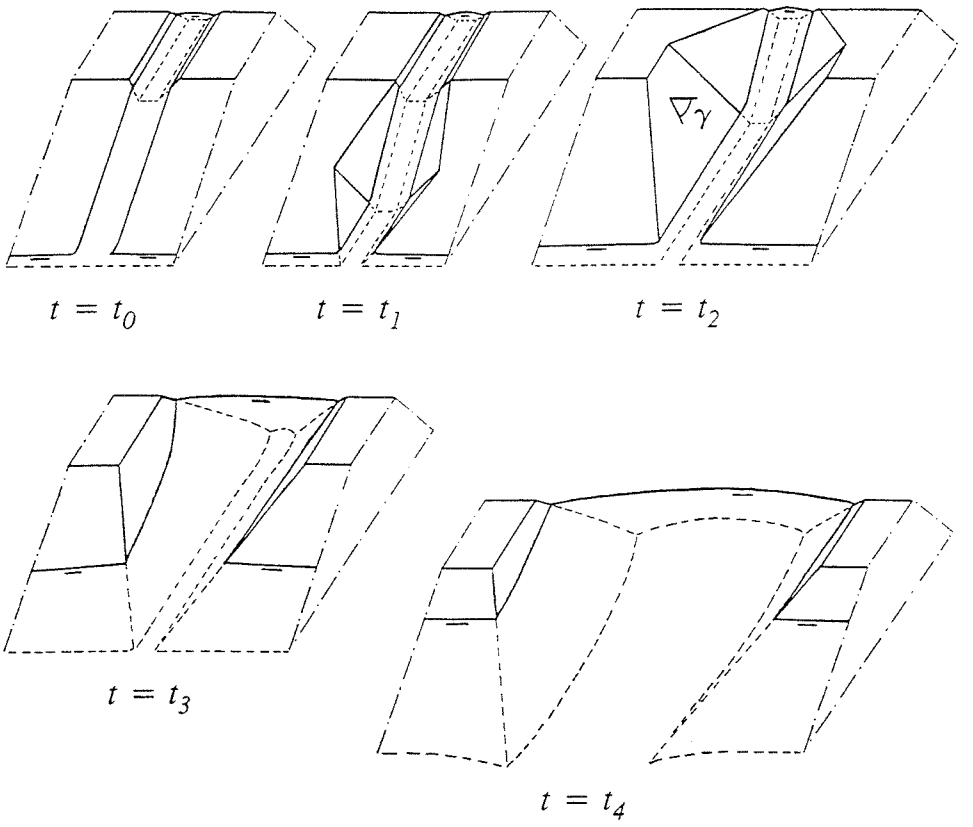

Fig. 2.1 Schematic illustration of breach growth in a sand-dike for $t_0 \leq t \leq t_4$.

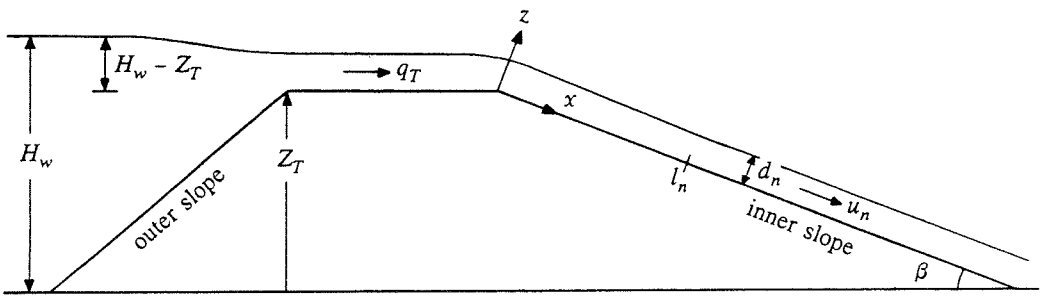

Fig. 2.2 Flow on a relatively steep sloping bed.

the breach has reached its maximum depth in the course of phase IV or V, the erosion of both side slopes of the breach dominates the continuation of the breaching process. The discontinuous sliding of large amounts of sand observed in the experiments indicates that this side slope erosion is controlled by the erosion at the toes of the side slopes. This means that the side slope angle plays also a fairly passive role in phases IV and V.

So it can be concluded that the effect of the side slope angle on the breach erosion process is of secondary importance. Therefore this study has been focused on sediment transport in flows on relatively steep slopes with the slope inclining in the flow direction.

Fig. 2.2 schematically shows the two-dimensional situation of flow on the relatively steep inner slope of a sand-dike (with angle of inclination β); x is the coordinate along the inner slope, z is the coordinate perpendicular to the slope, H_w is the water level against the dike and Z_T is the height of the dike-crown, both measured above the polder surface. The rate of discharge of the flow over the dike per unit breach width is q_T. Since the flow on the inner slope is supercritical, the equation for q_T is

$$q_T = m\frac{2}{3}(\frac{2}{3}g)^{1/2}H^{3/2} \tag{2.1}$$

where $H = H_w - Z_T$ and m is the discharge coefficient ($m \approx 1.0$), so it is assumed that the friction along the dike-crest is negligibly small. The water depth $d(0)$ for $x = 0$ is equal to the critical depth d_c, given by

$$d_c^{\,3} = \frac{q_T^{\,2}}{g} \tag{2.2}$$

The flow on the inner slope accelerates up to $x = l_n$, where the water depth d and the depth-averaged flow velocity u become equal to d_n and u_n, respectively:

$$d_n = \frac{(C\,q_T^{\,2})^{1/3}}{(g\sin\beta)^{1/3}} \tag{2.3}$$

$$u_n = \frac{(g\,d_n\sin\beta)^{1/2}}{C^{1/2}} = \frac{(g\,q_T\sin\beta)^{1/3}}{C^{1/3}} \tag{2.4}$$

in which C is a dimensionless friction coefficient (it is assumed that the bed shear stress τ_b can be written as $\tau_b = C\rho u^2$, where ρ is the water density) and d_n is the normal depth.

For $0 \le x \le l_n$ the general differential equation for gradually varied flow (equation of Bélanger) can be applied. For two-dimensional flows this equation reads

$$\frac{\mathrm{d}d}{\mathrm{d}x} = \frac{d^3 - d_n^{\,3}}{d^3 - d_c^{\,3}}\sin\beta \tag{2.5}$$

If the deviation between d and d_n is relatively small, then the following approximations hold:

$$d^3 - d_n^3 = (d - d_n)(d^2 + dd_n + d_n^2) \approx 3d_n^2(d - d_n) \tag{2.6}$$

$$d^3 - d_c^3 \approx d_n^3 - d_c^3 \tag{2.7}$$

Substitution of (2.6) and (2.7) into (2.5) gives

$$\frac{\mathrm{d}d}{\mathrm{d}x} = \frac{3(d_n - d)}{\lambda} \tag{2.8}$$

where

$$\lambda = \frac{d_c^3 - d_n^3}{d_n^2 \sin\beta} \tag{2.9}$$

Assuming λ to be constant, integration of (2.8) gives with the boundary condition $d = d(0)$ for $x = 0$:

$$d - d_n = \{d(0) - d_n\} e^{-3x/\lambda} \tag{2.10}$$

The parameter λ is a typical adaptation length for this type of gradually varied flow: for $x = \lambda$ the difference $d - d_n$ is about 5 % of the deviation $d(0) - d_n$ at $x = 0$ and for $x = 1.5\,\lambda$ it is only 1 %. Hence it can be assumed that $l_n \approx 1.5\lambda$, giving

$$l_n \approx \frac{1.5\,(d_c^3 - d_n^3)}{d_n^2 \sin\beta} \tag{2.11}$$

If $d_c^3 >> d_n^3$ then (2.11) reduces to

$$l_n \approx \frac{1.5\,d_c^3}{d_n^2 \sin\beta} = \frac{1.5\,q_T^{2/3}}{(C^2 g \sin\beta)^{1/3}} \tag{2.12}$$

The approximation for the water depth d along the stretch $0 < x < l_n$ reads

$$d \approx d_n + (d_c - d_n)\, \mathrm{e}^{-4.5x/l_n} \tag{2.13}$$

The sediment transport rate $s(x)$ per unit width along the inner slope consists of a part $s_b(x)$ that is transported in a relatively thin layer (some particle diameters thick) just above the bed and a part $s_s(x)$ that is transported in suspension:

$$s(x) = s_b(x) + s_s(x) \tag{2.14}$$

Sediment transport is here defined such that $s(x)$ contains only sediment and no voids; it is

expressed in units of volume of sediment per unit of time and per unit of breach width (SI: $(m^3/s)/m$). Whether the transport is in the suspended load mode or in the bed-load mode can be estimated with the parameter

$$\frac{u_\star}{w_s} = \sqrt{C}\frac{u}{w_s} \tag{2.15}$$

where $u_\star$ is the bed shear velocity, w_s is the sediment fall velocity and g is the acceleration of gravity. If $u_\star/w_s << 1$ (roughly $u_\star/w_s < 1$) then bed-load transport dominates suspended load transport. If $u/w_s >> 1$ (roughly $u/w_s > 2$) then most of the transport takes place as suspended load. Here $u_\star/w_s$ varies roughly between 7 and 25, so bed-load transport is small compared with suspended load transport.

It is assumed that the pick up of sediment and the resulting transport $s(x)$ starts at $x = 0$ at the top of the inner slope: $s(0) = 0$. This assumption is based on the laboratory observations of Visser (1988). The data of the Schelde Flume experiments (see Steetzel and Visser, 1992a, 1992b) support this assumption (see Figures 4.1 and 4.2). It is also assumed that the adaptation length of the bed-load transport is relatively small and that at $x = l_n$ the bed-load transport is equal to its equilibrium value (or transport capacity). At a distance l_a (is adaptation length of the suspended load transport) from $x=0$ the suspended load transport reaches its equilibrium value. There are various descriptions for the process of sediment entrainment. Among these is Galappatti's (1983) model, see also Galappatti and Vreugdenhil (1985). Galappatti's (1983) equation for suspended load transport reduces for large values of $u_\star/w_s$, as in the present situation, to a simple expression with which (2.14) reduces to

$$s(x) \approx s_b + \frac{x}{l_a} s_s \qquad \text{for} \quad l_n \le x \le l_a \tag{2.16}$$

where s_b and s_s are the equilibrium values of bed-load transport and suspended load transport, respectively (in next the subscripts b, s and t refer to equilibrium values of bed-load transport, suspended load transport and total load transport, respectively). The adaptation length l_a can roughly be approximated by (see Galappatti, 1983)

$$l_a \approx \frac{u\,d}{w_s \cos\beta} = \frac{q_T}{w_s \cos\beta} \tag{2.17}$$

The entrainment of sediment causes the flow rate $q(x)$ of the sand-water mixture to increase along the inner slope:

$$q(x) = q_T + s(x) \tag{2.18}$$

(it is assumed that the voids are filled with air and not with water). Under normal hydraulic conditions $s(x) << q(x)$ and the increase of the flow rate due to sediment entrainment can be neglected. In eroding breaches, however, the sediment transport can become relatively

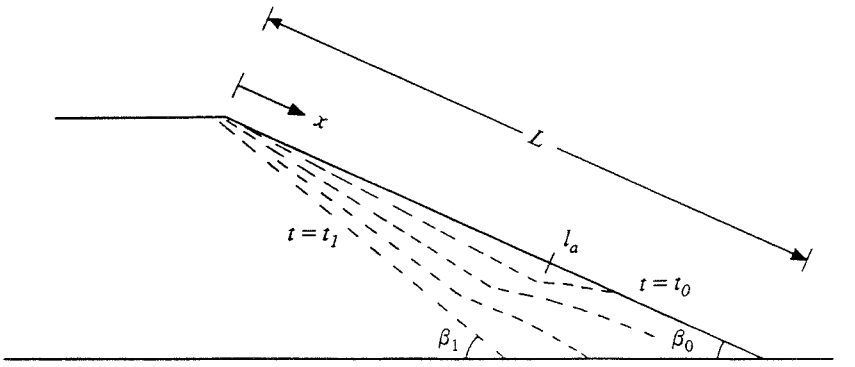

Fig. 2.3 Erosion inner slope if $L > l_a$.

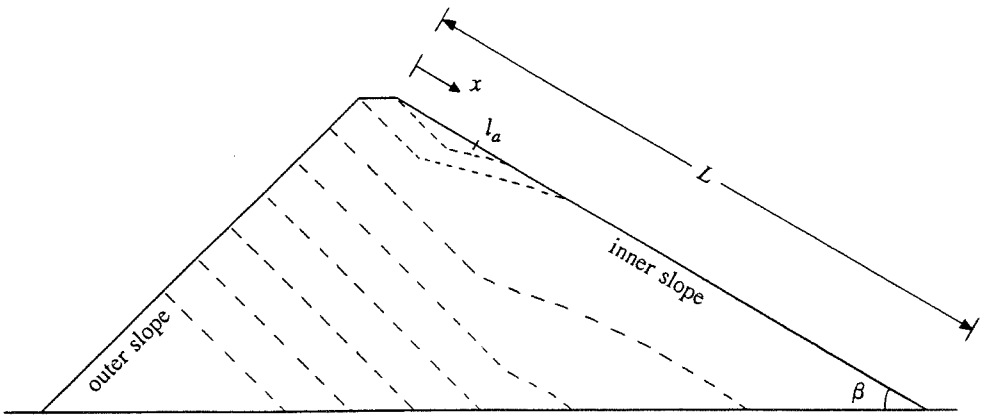

Fig. 2.4 Erosion inner slope if $L >> l_a$.

large (see chapter 4), and it may be important to account for this.

The scope of the present study is the investigation of the applicability of existing sediment transport formulae for use in breach erosion models. Therefore, the effect of an increase of $q(x)$ on u, d, l_a, etc. will be ignored, and will only be taken into account in the calculation of the depth-averaged sediment concentration c:

$$c(x) = \frac{s(x)}{q(x)} = \frac{s(x)}{q_T + s(x)} \tag{2.19}$$

Example: suppose $q_T = 0.2$ (m^3/s)/m, $s(0) = 0$ and $s(x_A) = 0.03$ (m^3/s)/m; this means that the amount of sediment picked up between $x = 0$ and $x = x_A$ is 0.03 (m^3/s)/m. The flow rate at $x = x_A$ is $q(x_A) = 0.23$ (m^3/s)/m and the depth-averaged concentration as defined above $c(x_A) = 0.13$, compared with a concentration $s(x_A)/q_T = 0.15$ if the increase of flow rate due to sediment entrainment is neglected.

If the length L of the inner slope is larger than the adaptation length l_a of the suspended load transport, then the increase in sediment transport rate stops at $x = l_a$ and consequently the erosion along $x > l_a$ also stops. After some time a bar will be formed at $x \approx l_a$ (see Fig. 2.3), causing a significant slow down of the supercritical flow, so also an increase of the turbulence intensity for $x \approx l_a$. More turbulence does increase the sediment transport capacity, which means that, with some delay, also the sediment downstream of $x = l_a$ will be removed (as observed in the Schelde Flume experiments, see Steetzel and Visser, 1992a, 1992b).

The removal of the sediment for $x \approx l_a$ is possibly not complete if $L >> l_a$, that is in case of very high dikes or very low flow rates q_T. It is thinkable that then the erosion of the inner slope takes place in two stages: in the first stage the top of the dike will be lowered (see Fig. 2.4), and the resulting larger flow rate removes the remaining sediment in the second stage.

The equilibrium values of the bed-load transport s_b and especially the suspended load transport s_s are important quantities in equation (2.16) for the sediment transport $s(x)$. Chapter 3 summarizes a number of available formulations for the equilibrium value of the sediment transport, both for bed-load transport and total load transport and total load transport consisting of bed-load transport and suspended load transport.

A parameter similar to u_*/w_s is Shields' particle mobility parameter, which reads

$$\theta = \frac{\tau_b}{\rho g \Delta D} = \frac{u_*^2}{g \Delta D} = \frac{Cu^2}{g \Delta D} \tag{2.20}$$

where $\Delta = (\rho_s - \rho)/\rho$ is the specific density, ρ_s is the sediment density and D is the averaged sediment particle diameter. The parameter θ is an important parameter in the sediment transport formulae in chapter 3, and somewhat less also its critical value (θ_{cr}), which is a

parameter for incipient motion.

Breach erosion is attended with large bed shear stresses, so large values for θ and high sediment concentrations (in particular near the bottom, see Fig. 3.1 and chapter 4). These high concentrations cause the viscosity of the flowing sand-water mixture to be much higher than that of water without sediment. This results in a relatively large value for the friction factor k in the equation for the bed friction coefficient:

$$C = \left[\frac{\kappa}{\ln(12d/k)} \right]^2 \tag{2.21}$$

Based on the experiments of Einstein and Chien (1955, see Van Rijn, 1993) and Winterwerp et al. (1990), Van Rijn (1993) proposed the following formulae for k:

$$k = 3D_{90} \quad \text{voor} \quad \theta < 1 \quad \text{(lower regime, plane bed)} \tag{2.22}$$

$$k = 3\theta D_{90} \quad \text{voor} \quad \theta \geq 1 \quad \text{(upper regime)} \tag{2.23}$$

Equation (2.23) is similar to the relation

$$k = 5\theta D_{50} \quad \text{voor} \quad \theta \geq 1 \tag{2.24}$$

proposed by Wilson (1989) and Wilson and Nnadi (1992). It can be concluded from (2.20), (2.21), (2.23) and (2.24) that for $\theta > 1$ the friction factor k is (almost) independent of the particle diameter D.

3 Available sediment transport formulae

This chapter summarizes the sediment transport formulations that have been included in the present study. Most of these formulations consist of one or two formula(e) (for example Engelund and Hansen, 1967); some formulations have a series of equations (for example Van Rijn, 1984a, 1984c).

The application range of the formulae in terms of Shields' mobility parameter (θ) and the Froude number (Fr) and experimental conditions as sediment diameter, bottom slope, flow velocity and sediment concentration are listed with the formulation if these are known. The absence of experimental verification is indicated by dashes.

The formulae give the equilibrium values for the rates of sediment transport expressed in amounts of volumes of sediment transport per unit of time per unit of (breach)width (SI-unit: $(m^3/s)/m$), that is without voids.

The equilibrium value for the sediment transport is given as bed-load transport (s_b), total sediment transport (s_t) or total sediment transport with a bed-load and a suspended load component ($s_t = s_b + s_s$). The conception of Mastbergen and Winterwerp (1987) differs from the other formulae in the sense that it is an erosion/deposition formulation and not a formula for the sediment transport capacity.

3.1 Formulae for sand-water mixture flows

3.1.1 Wilson (1966)

Bed-load transport:	$s_b = 12.1\,(g\Delta D^3)^{0.5}\,[\mu\theta - 0.047]^{1.5}$	(3.1)
Ranges of θ and Fr:	$1 < \mu\theta < 10$	
Sediment:	sand with diameter 0.4 - 1.3 mm ($D_{50} \approx 0.8$ mm) nylon particles with equivalent sphere diameter is 3.9 mm	
Slope angles:	horizontal, pressurized conduit	
Flow velocities:	-	
Concentrations:	high	

The parameter μ in equation (3.1) is the ripple factor ($\mu = 1$ for a plane bed). The solid particles in Wilson's (1966) experiments were generally transported in a 'dense layer immediately above the bed', 'supported by intergranular collision rather than by fluid turbulence'. Wilson (1966, 1992) has termed this bed-load transport, but since the thickness of the 'dense layer' in his experiments was much larger than a few particle diameters (as in Fig. 1), the term total sediment transport seems more in place.

For the empirical determination of (3.1), Wilson (1966) used only the data of his experiments with a plane bed and not his (small number of) experiments with ripples and dunes. This means for the ripple factor in (3.1) that $\mu = 1$.

Equation (3.1) is similar to the formula of Meyer-Peter and Müller (1948):

$$s_b = 8\,(g\Delta D^3)^{0.5}\,[\mu\theta - 0.047]^{1.5} \quad \text{for} \quad 0.03 < \mu\theta < 0.2 \tag{3.2}$$

Equation (3.2) has been derived using data from experiments in flumes with bed slopes: $0.0004 < \tan\beta < 0.02$, sand with a mean particle diameter D: $0.4\,\text{mm} < D < 29\,\text{mm}$, and a water depth d: $0.01\,\text{m} < d < 1.20\,\text{m}$.

Wilson (1966) argued that for $\mu\theta < 1$ equation (3.1) agrees almost as well with the data of Meyer-Peter and Müller (1948) as equation (3.2).

3.1.2 Wilson (1987)

Bed-load transport:	$s_b = 11.8\,(g\Delta D^3)^{0.5}\,\theta^{1.5} = 11.8\,\dfrac{(u_\star)^3}{g\Delta}$	(3.3)
Ranges of θ and Fr:	-	
Sediment:	13 mm gravel	
Slope angles:	horizontal, pressurized conduit	
Flow velocities:	see Fig. 3.1	
Concentrations:	see Fig. 3.1	

This publication is a sequel to Wilson (1966). Formula (3.3) has an empirical basis, just as (3.1). Fig. 3.1 shows 'data points for 13 mm gravel at a volumetric in situ solids concentration of 0.09 in a pipe of internal diameter 0.26 m. These data are typical of moderate concentrations of particles with large fall velocities, i.e., the upper portion of the flow is virtually particle-free, while the maximum concentration of particles, near the bottom of the pipe, approaches c_b. In between, the concentration decreases with height in an essentially linear fashion.' (after Wilson, 1987)

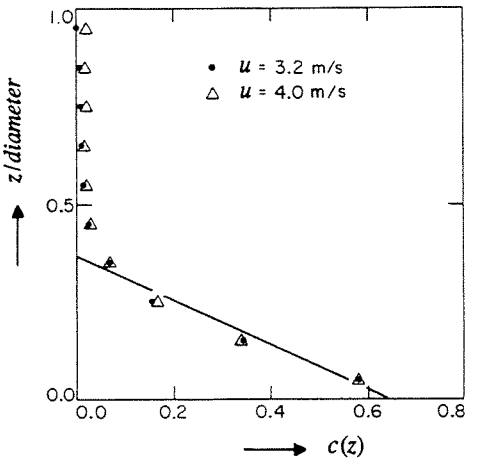

Fig. 3.1 Concentration profile measurements for coarse particle slurry in a pipe of internal diameter of 0.26 m (after Shook et al., 1982).

3.1.3 Mastbergen and Winterwerp (1987)

Sediment transport: $$s(x_1) = s(x_0) + (x_1 - x_0)(E - S_e) \tag{3.4}$$

where: $$E = 0.012 \frac{(g\Delta D)^{0.5} D^{0.3} (g\Delta/\nu^2)^{0.1} (\theta^{0.5} - 1.3)}{1 - \frac{\tan\beta}{\tan\phi}} \tag{3.5}$$

$$S_e = w_s c (1 - c)^4 \tag{3.6}$$

$$\theta = \frac{Cu^2}{g\Delta D} = 0.0125 \frac{u^2}{g\Delta D} \tag{3.7}$$

Ranges of θ and Fr: $3 < \theta < 24$

Sediment: sand, $0.12\,\text{mm} < D_{50} < 0.23\,\text{mm}$

Slope angles: $0.003 < \tan\beta < 0.4$

Flow velocities: -

Concentrations: $0 < c < 0.40$

E in (3.4) and (3.5) is the erosion rate and S_e in (3.4) and (3.6) is the sedimentation rate (E and S_e have the dimension of volume per unit of time and per unit of area [SI-unit: $(m^3/s)/m^2$]); ν is the kinematic viscosity and ϕ the angle of repose.

The formulation of Mastbergen and Winterwerp (1987) resulted from a study for the construction of the Philipsdam and the Oesterdam (part of Deltaworks in the Netherlands) with the sand-closure method, see also Winterwerp et al. (1990) and Winterwerp, et al. (1992).

Winterwerp et al. (1990) have described field experiments (during the construction of a sand dam closing the Slaak estuary) and laboratory experiments in a small sloping flume (length 1.5 m) and a larger sloping flume (length 9.0 m). The flow in the experiments was supercritical and the bed plane.

Winterwerp et al. (1990) presented a formula for the equilibrium bed slope above the water line at which sedimentation and erosion are in balance. 'For laminar flow conditions this slope is only dependent on the average sand concentration, whereas for turbulent conditions the flow rate per unit width (q) is the main parameter. The sand concentration near the bed (c_b) measured about 35% by volume for most test conditions. The vertical

gradient in sand concentration ($\partial c(z)/\partial z$) decreased with increasing mean sand concentration (c), indicating a decrease in the damping of turbulence. The velocity distribution ($u(z)$) behaved fairly logarithmically, showing a variation in slope with varying sand concentration. A minimum value of the effective von Karman constant ($\kappa \approx 0.2$) was found at concentrations of about 0.20. At high concentrations the viscous sublayer is thicker, resulting in a larger bed shear stress' (after Winterwerp et al., 1990).

In a sequel Winterwerp et al. (1992) have described situations with slopes slightly smaller than the equilibrium slope (yielding a sedimentation rate larger than the erosion rate). At these slopes, starting from a plane bed, sand bars will form. The supercritical flow over the upstream part of these bars decelerates and the sediment transport capacity decreases. The deceleration can be so large that a hydraulic jump is formed upstream of the bar. 'The flow is now subcritical up to the crest of the bar. Beyond the crest on the lee side of the bar, the flow accelerates, becoming supercritical again.' A bar consists of a nearly horizontal terrace with subcritical flow, a steep lee side with supercritical flow and a hydraulic jump in between. 'On the subcritical part of the bar, net sedimentation will occur; at the lee side net erosion. Because of this a bar moves upstream. Thus, a cascade of sandbars can be formed, propagating upstream, resembling 'the behaviour of antidunes and chute-pool systems. According to the classical regime theory, these bed forms can develop at high Froude numbers and low Shield numbers[1], see Kennedy (1969), Engelund (1970) and Allen (1982)', after Winterwerp et al. (1992).

The erosion rate at the lee side of the bar was generally limited due to the large concentrations and, according to Winterwerp et al. (1992), more moderate than predicted by the pick-up functions used in classical sediment transport theory (see Van Rijn, 1984b). The high concentrations did also restrict the sedimentation, described in (3.6) by the factor $(1-c)^4$, termed 'hindered settling'.

The value 0.0125 for the friction coefficient C, see equation (3.7), approaches the value measured in the field experiments in the Slaak estuary (construction of Philipsdam), see also chapter 4.

Mastbergen and Winterwerp (1987) and Winterwerp et al. (1992) schematized the cascade of antidunes as a series of triangles and introduced the erosion/deposition function (3.4) with (3.5), (3.6) and (3.7) to describe the physics of such a chute-pool system. Winterwerp et al. (1992) claimed that the agreement with the experimental data is reasonable.

---

[1] Generally the Shields number is very large in the first stages of the sand-dike breaching process, see chapter 4.

3.2 Formulae for sediment transport on steep slopes

3.2.1 Mizuyama (1977)

Bed-load transport over a plane bed:

$$s_b = (g\Delta D^3)^{0.5} \frac{12 - 24(\tan\beta)^{0.5}}{\cos\beta} \theta^{1.5 - (\tan\beta)^{0.5}} (1 - \xi^2 \frac{\theta_{cr}}{\theta}) (1 - \xi (\frac{\theta_{cr}}{\theta})^{0.5}) \qquad (3.8)$$

where: $$\xi^2 = \frac{0.85(1 - \rho/\rho_s) - 2\tan\beta}{1 - \rho/\rho_s - \tan\beta} \qquad (3.9)$$

Ranges of θ and Fr: -

Sediment: -

Slope angles: $0.05 < \tan\beta < 0.2$

Flow velocities: -

Concentrations: -

θ_{cr} in (3.8) is the critical value of θ, at which incipient motion takes place, see Fig. 3.2 (page 18). Throughout this report the subscript *cr* refers to the critical value at initiation of motion.

The dissertation of Mizuyama (1977) has been written in Japanese; the above description of Mizuyama's formula has been adopted from publications of Jaeggi and Rickenmann (1987) and Takahashi (1987). These papers do not include information about the validity range (θ, Fr) of the formula or about the sediment, flow velocities and concentrations.
Ashida et al. (1978) have written (3.8) for $0.02 < \tan\beta < 0.1$ as:

$$s_b = (g\Delta D^3)^{0.5} \frac{12 - 24(\tan\beta)^{0.5}}{\cos\beta} \theta^{1.5} (1 - \xi^2 \frac{\theta_{cr}}{\theta}) (1 - \xi (\frac{\theta_{cr}}{\theta})^{0.5}) \qquad (3.10)$$

see Takahashi (1987).

Note that (3.8) is restricted to $\tan\beta < 0.2$. Application of formula (3.8) to breach erosion is in general not possible due to the steep slopes occurring in this process (for $\tan\beta > 0.25$, (3.8) predicts negative values of s_b).

3.2.2 Smart and Jaeggi (1983)

Bed-load transport:

$$s_b = 4\,C^{-0.5}\,(g\Delta D^3)^{0.5}\left[\frac{D_{90}}{D_{30}}\right]^{0.2}(\tan\beta)^{0.6}\,\theta^{0.5}[\theta - \theta_{cr}(\beta)] \tag{3.11}$$

where: $$\theta_{cr}(\beta) = \theta_{cr}\cos\beta\left[1 - \frac{\tan\beta}{\tan\phi}\right] \tag{3.12}$$

Ranges of θ and Fr:	$0.1 < \theta < 3.3$ $\quad 1.1 < Fr < 3.3$
Sediment:	sand, $0.4\,\text{mm} < D < 29\,\text{mm}$ and $D_{90}/D_{30} < 8.5$
Slope angles:	$0.03 < \tan\beta < 0.2$
Flow velocities:	$0.8\,\text{m/s} < u < 2.0\,\text{m/s}$
Concentrations:	$0.006 < c < 0.19$

Equation (3.11) has resulted from Smart en Jaeggi's (1983) experimental investigation in the laboratory into the sediment transport capacity of flows on relatively steep slopes, see also Smart (1984) and Rickenmann (1991). Smart and Jaeggi calibrated (3.11) also to the old data of Meyer-Peter and Müller (1948), for which $0.0004 < \tan\beta < 0.02$. The parameter D_{90}/D_{30} in (3.11) represents the effect of non-uniform sand.

A test of the original formula of Meyer-Peter and Müller (1948) to Smart and Jaeggi's new data has shown that the MPM formula underestimates the transport capacity for slopes with $\tan\beta > 0.03$.

3.2.3 Bathurst, Graf and Cao (1987)

Bed-load transport:	$s_b = 2.5 \frac{\rho}{\rho_s} (\tan\beta)^{3/2}(q - q_{cr})$	(3.13)
where:	$q_{cr} = 0.21\, g^{0.5} (D_{16})^{1.5} (\tan\beta)^{-1.12}$	(3.14)
Ranges of θ and Fr:	$0.1 < \theta < 0.4$ $\quad 0.3 < Fr < 2.2$	
Sediment:	$12\,\text{mm} < D_{50} < 44\,\text{mm}$	
Slope angles:	$0.005 < \tan\beta < 0.09$	
Flow velocities:	-	
Concentrations:	$0 < c < 0.03$	

Bathurst et al. (1987) have termed (3.13) a modified Schoklitsch formula, see Schoklitsch (1962). The confrontation of (3.13) with experimental data has indicated that (3.13) underestimates the sediment transport capacity for $\theta > 0.4$ and for $\tan\beta < 0.01$ and $\tan\beta > 0.1$ (see Bathurst et al., 1987).

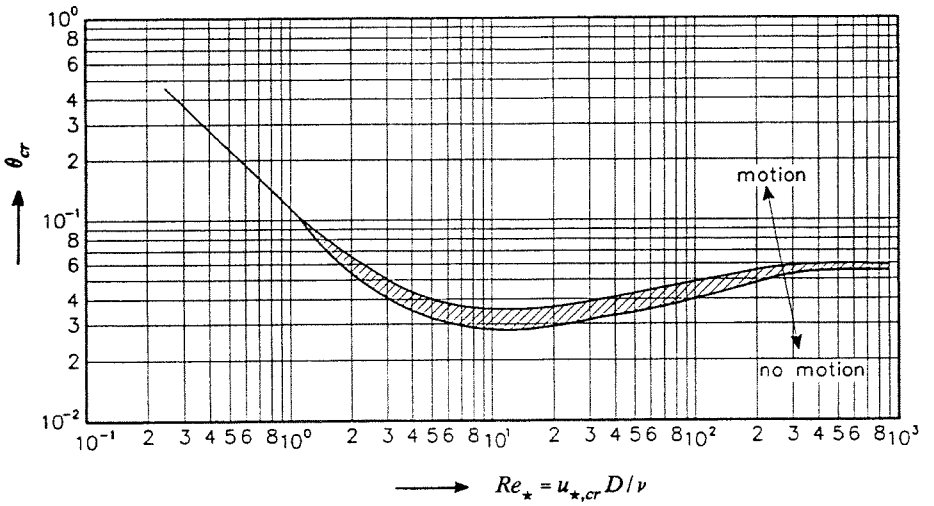

Fig. 3.2 Initiation of motion for a current over a plane, weakly sloping bed according to Shields (1936), $\theta_{cr} = f(Re_*)$; after Van Rijn (1993).

3.2.4 Takahashi (1987)

Bed-load transport:

$$s_b = C^{-0.5}(g\Delta D^3)^{0.5}\,\frac{1+5\tan\beta}{\cos\beta}\,\theta^{1.5}\,(1-\xi^2\frac{\theta_{cr}}{\theta})\,(1-\xi(\frac{\theta_{cr}}{\theta})^{0.5}) \qquad (3.15)$$

where: $$C^{-0.5} = A + 5.75\log\left(\frac{\Delta\theta}{(1+2\theta)\sin\beta}\right) \quad \text{for } \theta \geq 0.2 \qquad (3.16)$$

$$C^{-0.5} = A + 5.75\log\left(\frac{0.14\Delta}{\sin\beta}\right) \quad \text{for } \theta < 0.2 \qquad (3.17)$$

with: $$A = \frac{0.04}{(\sin\beta)^2} \quad \text{for } \sin\beta > 0.08 \qquad (3.18)$$

$$A = 6 \quad \text{for } \sin\beta \leq 0.08 \qquad (3.19)$$

and: $$\xi^2 = \frac{0.85(1-\rho/\rho_s) - 2\tan\beta}{1-\rho/\rho_s - \tan\beta} \qquad (3.9)$$

Ranges of θ and Fr: $0.1 < \theta < 4$

Sediment: -

Slope angles: $0.03 < \tan\beta < 0.20$

Flow velocities: -

Concentrations: -

Takahashi (1987) derived (3.15) empirically using the data of Ashida et al. (1978) and Smart and Jaeggi (1983). Takahashi (1987) concluded that (3.15) gives better agreement with the data than (3.10) and (3.11). It can be seen from (3.9) that as $\rho_s/\rho = 2.65$ then ξ^2 is negative for $\beta > 14°$.

3.2.5 Rickenmann (1991)

Bed-load transport in water and in clay suspensions:

$$s_b = 12.6\Delta^{-1.6}\left[\frac{D_{90}}{D_{30}}\right]^{0.2}(\tan\beta)^2(q - q_{cr}) \tag{3.20}$$

where: $q_{cr} = 0.065\Delta^{1.67}g^{0.5}(D_{50})^{1.5}(\tan\beta)^{-1.12}$ (3.21)

Ranges of θ and Fr:	$0.1 < \theta < 3.3$ $\quad 1.5 < Fr < 2.8$
Sediment:	sand, $0.4\,\text{mm} < D < 29\,\text{mm}$ and $D_{90}/D_{30} < 8.5$ (sand in clear water), gravel, $D = 1.0\,\text{cm}$ and $D_{90} = 1.2\,\text{cm}$ (debris flow: gravel in clay suspension)
Slopes:	$0.03 < \tan\beta < 0.20$
Flow velocities:	$0.8\,\text{m/s} < u < 2.0\,\text{m/s}$
Concentrations:	$0.006 < c < 0.19$
Density clay-suspension:	$998\,\text{kg/m}^3 < \rho_{susp} < 1246\,\text{kg/m}^3$

Equation (3.20) has resulted from an analysis of data of experiments on bed-load transport on relatively steep slopes, i.e. Smart and Jaeggi's (1983) experiments, and Rickenmann's (1991) experiments with clay suspensions (only those experiments with negligible viscous effects).

Rickenmann (1991) presented also an empirical transport formula, valid for both mild and steep slopes (i.e. $0.001 < \tan\beta < 0.20$):

$$s_b = 3.1\,\frac{(g\Delta D^3)^{0.5}}{\Delta^{0.5}}\left[\frac{D_{90}}{D_{30}}\right]^{0.2}\theta^{0.5}[\theta - \theta_{cr}(\beta)]Fr^{1.1} \tag{3.22}$$

3.3 Formulae for total sand transport in river regimes

3.3.1 Engelund and Hansen (1967)

Total load transport:	$s_t = 0.05\, C^{-1} (g \Delta D_{50}{}^3)^{0.5}\, \theta^{2.5}$	(3.23)
Ranges of θ and Fr:	$0.07 < \theta < 6$ $\quad 0.1 < Fr < 0.8$	(Voogt et al., 1991)
Sediment:	sand, $0.19\,\text{mm} < D < 0.93\,\text{mm}$	
Slope angles:	$\tan\beta < 0.005$	(Voogt et al., 1991, estimated)
Flow velocities:	$u < 2.8\,\text{m/s}$	(Voogt et al., 1991)
Concentrations:	$c_b < 0.04$, $c < 0.0004$	(Voogt et al., 1991)

Engelund and Hansen (1967) tested their formula to the experimental data of Guy et al. (1966) for $0.07 < \theta < 6$. The effect of the sloping bed has not explicitly been taken into account in the derivation and test of their formula.

Voogt et al. (1991) tested Engelund and Hansen's formula for relatively large flow velocities to the data of Peterson and Howells (1973), the data of the measurements of Van Rijn (1985) in a laboratory flume and to the data of field measurements (on a sandy sill during the construction of the Philipsdam). The main features of these experiments are: subcritical flow, sand with a diameter between 0.1 mm and 0.4 mm, depth-averaged flow velocities (u) and values for the mobility parameter (θ) and the Froude number (Fr) as indicated above.

3.3.2 Van Rijn (1984a, 1984c)

Total load transport:	$s_t = s_b + s_s$ (see next page)	(3.24)
Ranges of θ and Fr:	$\theta < 6$ $0.1 < Fr < 0.8$ (Voogt et al., 1991)	
Sediment:	sand with diameter between 0.09 mm and 2.0 mm	
Slope angles:	$\tan\beta < 0.005$ (Voogt et al., 1991, estimated)	
Flow velocities:	$u < 2.8$ m/s (Voogt et al., 1991)	
Concentrations:	$c_b < 4\,\%$ $c < 0.04\,\%$ (Voogt et al., 1991)	

Van Rijn (1984a, 1984c) tested his formulae for bed-load and suspended load transport to a large number of experimental data from the field and the laboratory. The slope effect has not been explicitly taken into account in this formulae.

Van Rijn's formulation for the total transport capacity holds a large number of formulae, which are reproduced on the next page. The following symbols still need to be defined: T is the transport stage parameter, $D_\star$ is a dimensionless particle parameter, $u_\star'$ is the bed-shear velocity related to grains and a is a reference level above the bed, where the sediment concentration is c_a. The factor n in (3.33) is of order 10.

Voogt et al. (1991) tested Van Rijn's formulation for relatively large flow velocities with the data mentioned in section 3.3.1. The flow in these experiments was subcritical, the sand had a diameter between 0.1 mm and 0.4 mm and depth-averaged flow velocities (u) and values for the mobility parameter (θ) and Froude number (Fr) as given above. Voogt et al. (1991) concluded that Van Rijn's formulation gives reasonable good agreements with the experimental data (somewhat better than Engelund and Hansen's formula).

3.3.2 Van Rijn (1984a, 1984c), continuation

Bed-load transport:

$$s_b = 0.053\,(g\Delta D_{50}^{\,3})^{0.5}\,\frac{T^{2.1}}{(D_\star)^{0.3}} \qquad \text{for} \quad T < 3 \tag{3.25}$$

$$s_b = 0.1\,(g\Delta D_{50}^{\,3})^{0.5}\,\frac{T^{1.5}}{(D_\star)^{0.3}} \qquad \text{for} \quad T \geq 3 \tag{3.26}$$

where:

$$T = \frac{(u_\star')^2 - (u_{\star,cr})^2}{(u_{\star,cr})^2} \tag{3.27}$$

$$u_\star' = \frac{\kappa u}{\ln(12d/3D_{90})} \leq u_\star \tag{3.28}$$

$u_{\star,cr}$ = critical $u_\star$ (given by θ_{cr}, see Fig. 3.3)

$$D_\star = D_{50}\,(g\Delta/\nu^2)^{1/3} \tag{3.29}$$

Suspended load transport:

$$s_s = F\,u\,d\,c_a \tag{3.30}$$

where:

$$F = \frac{(a/d)^{Z'} - (a/d)^{1.2}}{(1 - a/d)^{Z'}\,(1.2 - Z')} \tag{3.31}$$

$$Z' = \frac{w_s}{\left(1 + 2\,(w_s/u_\star)^2\right)\kappa u_\star} + 2.5\left[\frac{w_s}{u_\star}\right]^{0.8}\left[\frac{c_a}{c_0}\right]^{0.4}$$

$$\text{for} \quad 0.01 < \frac{w_s}{u_\star} < 1 \quad , \quad \frac{c_a}{c_0} \leq 1 \tag{3.32}$$

$$a = k \qquad \text{with} \quad 0.01d \leq a < 0.3d \quad (a < nD_{90}) \tag{3.33}$$

$$c_a = 0.015\,\frac{D_{50}}{a}\,\frac{T^{1.5}}{(D_\star)^{0.3}} \tag{3.34}$$

c_0 = sediment concentration in bed (= 0.6 here)

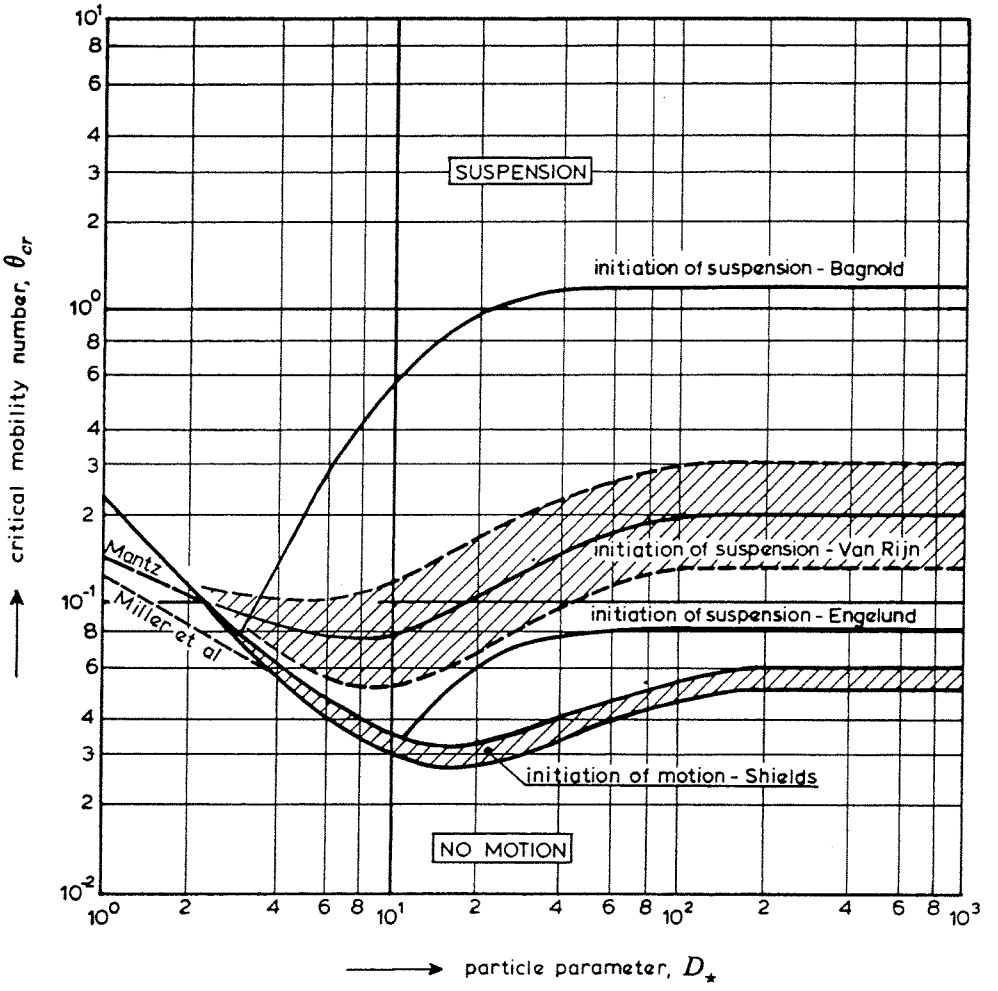

Fig. 3.3 Initiation of motion and suspension for a current over a plane, weakly sloping bed, $\theta_{cr} = f(D_*)$; after Van Rijn (1993).

3.4 Energetics-based formulae

3.4.1 Bagnold (1963, 1966)

Total load transport: $s_t = s_b + s_s$ (3.24)

where: $s_b = \frac{0.13}{\tan\phi - \tan\beta} \frac{Cu^3}{\Delta g}$ $(\beta < \phi)$ (3.35)

$s_s = \frac{0.01}{w_s/u - \tan\beta} \frac{Cu^3}{\Delta g}$ $(\tan\beta < w_s/u)$ (3.36)

Ranges of θ and Fr: -

Sediment: -

Slope angles: -

Flow velocities: -

Concentrations: -

Bagnold's energetics-based sediment transport model distinguishes two distinct modes for the sediment transport, each differing by way of the support of the sediment grains. Particles transported as bed-load are supported by the bed via the grain-grain interactions. Grains transported as suspended load are supported by the stream via turbulent diffusion. In both modes, energy is expended by the stream in transporting the sediment load.

Bagnold defined the sediment transport efficiency as the ratio of the rate of energy expenditure in transporting either the bed-load or the suspended load, divided by the total rate of energy production of the stream. If ω is the rate of energy production by the stream ($\omega = \tau_b u$), then $e_b \omega$ is used for the bed-load transport and $e_s(1-e_b)\omega = e\omega$ for the suspended load transport (e_b is the bed-load efficiency, e_s is the suspended load efficiency, $e_b \approx 0.13$ and $e \approx 0.01$ according to Bagnold, 1966). Bagnold determined the values for the efficiency coefficients e_b and e in a semi-empirical way.

3.4.2 Yang (1979)

Total load transport:

$$\log c_{tw} = 5.165 - 0.153 \log\left[\frac{w_s D}{\nu}\right] - 0.297 \log\left[\frac{u_\star}{w_s}\right] +$$

$$+ \left[1.780 - 0.360 \log\left[\frac{w_s D}{\nu}\right] - 0.480 \log\left[\frac{u_\star}{w_s}\right]\right] \log\left[\frac{u \sin\beta}{w_s}\right] \qquad (3.37)$$

where c_{tw} is the total bed-material sand concentration in parts per million by weight

Ranges of θ and Fr: -

Sediment: sand (not gravel)

Slope angles: -

Flow velocities: -

Concentrations: $c_{tw} > 100$ ppm ($= [g/m^3]$)

In two other publications Yang has presented similar formulae for the transport of sand close to incipient motion and for the transport of gravel, respectively, see Yang and Kong (1991).

The dimension of c_{tw} is [ppm] by weight (SI-unit: [10^{-3} kg] sediment per [10^3 kg] water, or [10^{-3} kg/m^3]). The equation for the corresponding concentration by volume (c_t) is:

$$c_t = 10^{-3} \frac{c_{tw}}{\rho_s} \quad [-] \qquad (3.38)$$

3.4.3 Bagnold-Bailard (1981)

Total load transport: $s_t = s_b + s_s$ (3.24)

where: $s_b = \dfrac{0.13}{\tan\phi - \tan\beta}\dfrac{Cu^3}{\Delta g} \quad (\beta < \phi)$ (3.35)

$s_s = \dfrac{0.01}{w_s/u - 0.01\tan\beta}\dfrac{Cu^3}{\Delta g} \quad (0.01\tan\beta < w_s/u)$ (3.39)

Ranges of θ and Fr: -

Sediment: -

Slope angles: -

Flow velocities: -

Concentrations: -

Bailard (1981) adopted Bagnold's formula (3.35) for the bed-load capacity without any change. Equation (3.39) differs from Bagnold's (3.36) by the inclusion of the factor $e \approx 0.01$ in the denominator. This difference arises because Bailard assumed that the stream power contribution from the suspended sediment load (owing to a gravity slope $\tan\beta$) contributes not directly to the suspended sediment transport rate as in (3.36) but through the efficiency e.

3.4.4 Bagnold-Visser (1988)

Total load transport: $s_t = s_b + s_s$ (3.24)

where: $$s_b = \frac{0.13}{(\tan\phi - \tan\beta)\cos\beta}\frac{Cu^3}{\Delta g} \quad (\beta < \phi) \tag{3.40}$$

$$s_s = \frac{0.01}{(w_s/u)(\cos\beta)^2}\frac{Cu^3}{\Delta g} = \frac{0.01\,Cu^4}{\Delta g w_s(\cos\beta)^2} \tag{3.41}$$

$$s_b/s_s \approx 0 \quad \text{if} \quad u_\star/w_s >> 1 \tag{3.42}$$

Ranges of θ and Fr: $11 < \theta < 106$ $2.8 < Fr < 4.1$ (this investigation)

Sediment: sand, $D_{50} = 0.10$ mm and $D_{50} = 0.22$ mm

Slope angles: $0.36 < \tan\beta < 0.62$ (this investigation)

Flow velocities: $1.2\,\text{m/s} < u < 3.5\,\text{m/s}$ (this investigation)

Concentrations: $0.007 < c < 0.28$ (this investigation)

The difference between (3.40) and (3.35) is the term $\cos\beta$ in the denominator of (3.40). This difference originates from the definition by Bagnold (1963) of the 'dynamic transport rate' (immersed weight of sediment in water column multiplied with transport velocity multiplied with $\cos\beta$). In practice the difference is not relevant: also for somewhat larger slopes is $\cos\beta \approx 1$, and as $\beta \to \phi$, then both (3.35) and (3.40) predict very large amounts of bed-load transport which cannot actually occur.

The difference between (3.41) and (3.36) is more significant. Visser (1988) argued that the existence of a power gradient in the flow direction (owing to a gravity slope $\tan\beta$) does not reduce the work done by the fluid in a situation where erosion predominates and neglected this term.

For $\beta \to 0$ both (3.39) and (3.41) reduce to Bagnold's (1963, 1966) original (3.36).

3.5 Takahashi's (1991) formula for immature debris flow

Total load transport:

$$s_t = \frac{2.8 - 0.2c_0}{(\tan\phi - \tan\beta)^2(\cos\beta)^2}(g\Delta D^3)^{0.5}\theta^{2.5} \qquad (\beta < \phi) \tag{3.43}$$

Ranges of θ and Fr:	$0.4 < \theta < 3$
Sediment:	-
Slope angles:	$0.07 < \tan\beta < 0.18$
Flow velocities:	-
Concentrations:	$0.1 < c < 0.20$

Debris flows are flows of sediment-water mixtures, in which the solid fraction consists of mud or sand or gravel or large stones or a mixture of these sediments, and in which the sediment concentrations are relatively high ($0.1 < c < 0.55$). Debris flows occur on relatively steep slopes in mountainous areas, mostly after heavy rainfall. Debris flows have occasionally caused great damage (including many lives) to communities at the foot of mountains.

Takahashi (1991) has discriminated different types of debris flows: A. stony debris flows, B. immature debris flows, C. turbulent debris flows and D. hybrid of stony and muddy debris flows. Fig. 3.4 (after Takahashi, 1991) shows the existence domain in terms of the parameters $(\sin\beta)/\Delta$ en d/D for the various types of debris flows. For the present experimental situations: $0.19 < (\sin\beta)/\Delta < 0.32$ and $38 < d/D < 320$, i.e. according Fig. 3.4 in and beyond the turbulent mud flow range. However, for turbulent mud flows Takahashi (1991) presented only equations for u (and the distribution of the flow velocity normal to the sloping bed) as function of a given concentration c (and not an erosion function or transport formula), which is not sufficient for the present application.

Fig. 3.5 (after Takahashi, 1991) shows that in immature debris flows the solids are concentrated in the lower part of the flow. This is exactly what has been observed in the breach erosion experiments in the laboratory by Visser (1988) and Steetzel en Visser (1992a, 1992b). The stony debris flows and the turbulent debris flows are mature, so with sediment throughout the entire vertical. The hybrid of stony and muddy debris flows can be both mature and immature.

Takahashi (1991) has given only a transport formula for immature debris flows, and not for the types A, C en D. So only this formula is available for the present comparison.

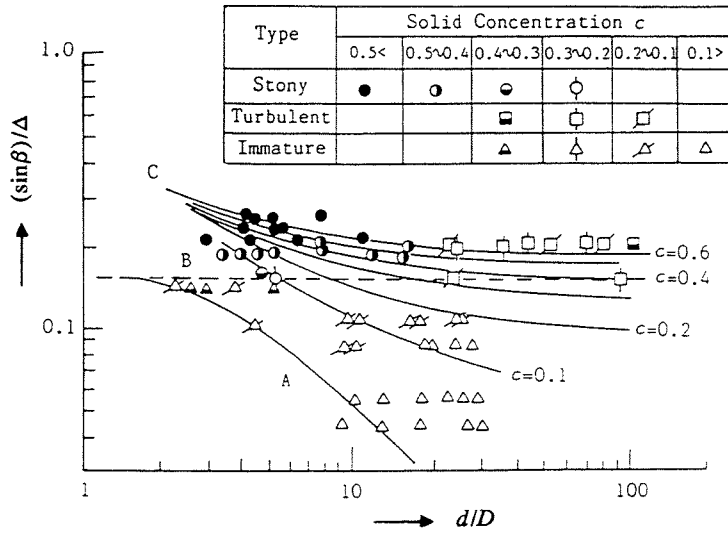

Fig. 3.4 Existence domain of various debris flows (Takahashi, 1991).

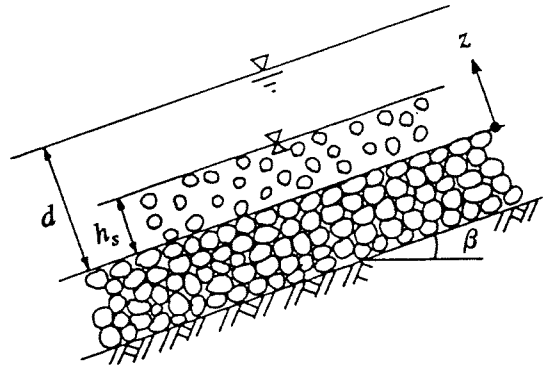

Fig. 3.5 Schematic illustration of the immature debris flow (Takahashi, 1991).

4 Comparisons with experimental results

4.1 Introduction

The available sediment transport formulations summarized in chapter 3 are compared with the data of three experiments: the laboratory experiments T3 and T5A of the TAW experiments in the Schelde flume (see Steetzel and Visser, 1992a, 1992b) and the Zwin'89 field experiment in the Zwin Channel (see Visser et al., 1990).

The Schelde flume (located in Delft Hydraulics' 'De Voorst' department) is 50 m long; its width is 1.00 m, and its depth is 1.20 m. A total number of nine tests were done to measure the 2DV-development of a breach in a 0.70 m high sand-dike along the breach axis. The observations of profile development were done by means of video. The role of the sediment particle diameter was included by using sand with a $D_{50} = 0.10$ mm (as in experiment T3) and sand with a $D_{50} = 0.22$ mm (as in experiment T5A).

The Zwin Channel is a tidal inlet, located at the Netherlands-Belgium border, that connects 'Het Zwin' (a nature reserve) with the North Sea. At high water the width of the inlet is about 200 m. A sand-dam was built, exclusively for the field experiment, at low water with local sand. The 2.2 m high dam temporarily closed the Zwin Channel.

4.2 Experimental conditions

4.2.1 Schelde Flume experiment T3

The dike in this experiment was constructed with sand with $D_{50} = 0.10$ mm ($D_{10} = 0.069$ mm, $D_{90} = 0.15$ mm). The mean fall velocity of this sediment at a water temperature $T \approx 16°C$ is $w_s = 0.0090$ m/s. At the start of the experiment (at $t = t_0 = 0$ s), the cross-section of the sand-dam had the following dimensions: top height above the flume bottom $Z_T = 0.70$ m, a crest width of 1.3 m, inclination angle of inner slope $\beta_0 = 18°$ (slope 1 in 3), length inner slope $L_0 = 2.2$ m and inclination angle of outer slope 1 : 30 (schematized dune erosion profile). The length of the dike was 0.40 m (equal to the effective width of the flume at the dam).

The outer water level H_w (measured above the bottom of the flume) was maintained as long as possible at $H_w = 0.75$ m by pumping back the water from the downstream to the up-stream end of the flume. According to the weir formula (2.1), a water head $H_w - Z_T = 0.05$ m over the sand-dam gives a flow discharge $q_T = 0.019$ (m^3/s)/m over its crest. Bed friction

	Schelde Flume experiments						Zwin'89 exp.	
	T3		T5A					
T [°C]	16						5	
ν [m^2/s]	$1.1 * 10^{-6}$						$1.5 * 10^{-6}$	
D_{50} [mm]	0.10		0.22				0.22	
w_s [m/s]	0.0090		0.028				0.024	
t [s]	10	30	10	30	100	240	45	240
q_T [m^3/s/m]	0.015	0.015	0.015	0.015	0.010	0.18	0.10	0.25
d_c [m]	0.028	0.028	0.028	0.028	0.022	0.15	0.10	0.18
u_c [m/s]	0.53	0.53	0.53	0.53	0.46	1.2	1.0	1.4
$C(0) * 10$ [-]	0.036	0.036	0.045	0.045	0.049	0.028	0.031	0.029
$\theta(0)$ [-]	0.62	0.62	0.35	0.35	0.29	1.2	0.85	1.45
β [°]	20	23	20	28	32	32	25	32
$C(l_n)$ [-]	0.025	0.027	0.022	0.028	0.032	0.032	0.026	0.032
d_n [m]	0.012	0.012	0.011	0.011	0.0085	0.058	0.040	0.072
u_n [m/s]	1.3	1.3	1.3	1.3	1.2	3.1	2.5	3.4
$\theta(l_n)$ [-]	24	28	11	14	12	85	46	106
l_n [m]	0.67	0.60	0.72	0.55	0.38	2.6	2.1	3.2
l_a [m]	1.8	1.8	0.72 (0.57)	0.61	0.42	7.6	4.6	12
L [m]	2.0	1.9	2.2	2.2	1.3	1.0	4.4	3.5
$d(L)$ [m]	d_n					0.074	d_n	
$u(L)$ [m/s]	u_n					2.4	u_n	
$C(L) * 10$ [-]	$C(l_n) * 10$					0.089	$C(l_n) * 10$	
$\theta(L)$ [-]	$\theta(l_n)$					15	$\theta(l_n)$	

Table 4.1 Data of the eight cases of the Schelde Flume experiments and the Zwin'89 experiment that have been applied to the test of the various sediment transport formulae (measured parameters: T, D_{50}, q_T, β and L; calculated parameters: d_c, u_c, $C(0)$, $\theta(0)$, $C(l_n)$, d_n, u_n, $\theta(l_n)$, l_n, l_a, $d(L)$, $u(L)$, $C(L)$ and $\theta(L)$, calculated as described in section 4.2).

along the mild outer slope and the horizontal crest, caused q_T to be smaller for $0 < t < 100$ s: $q_T \approx 0.015$ (m^3/s)/m (see Steetzel and Visser, 1992a).

Fig. 4.1 shows the development of the cross-section in this experiment (observed from the video-images). The sediment transport rates at times $t = 10$ s and $t = 30$ s ($\approx t_1$) have been determined from these profiles by assessing amounts of eroded sediment between $t = 0$ s and $t = 20$ s and between $t = 20$ s and $t = 40$ s and dividing these amounts by $\Delta t = 20$ s (see section 4.3).

The water depth $d(0)$ and flow velocity $u(0)$ at the top of the inner slope ($x = 0$) can be calculated with (2.2): $d(0) = d_c = 0.028$ m, $u(0) = u_c = 0.53$ m/s as $q_T = 0.015$ (m^3/s)/m. Equations (2.20), (2.21) and (2.22) give for $x = 0$ a friction coefficient $C(0) = 0.0036$ and a mobility parameter $\theta(0) = 0.62$.

The flow on the inner slope accelerated between $x = 0$ and $x = l_n$. If $q_T = 0.015$ (m^3/s)/m and $\beta \approx 20°$ (see Fig. 4.1), then (2.3), (2.4), (2.11), (2.20), (2.21) and (2.23) yield: $C(l_n) = 0.025$, $\theta(l_n) = 24$, $d_n = 0.012$ m, $u_n = 1.3$ m/s and $l_n = 0.67$ m at $t = 10$ s (as $L \approx 2.0$ m, see Fig. 4.1). Identically for $t = 30$ s (as $\beta \approx 23°$ and $L \approx 1.9$ m, see Fig. 4.1): $C(l_n) = 0.027$, $\theta(l_n) = 28$, $d_n = 0.012$ m, $u_n = 1.3$ m/s and $l_n = 0.60$ m.

The calculated values for l_n are estimated values. First of all (2.11) gives an overestimation of l_n (see chapter 2). Besides, calculating l_n with (2.11) it is assumed that $C = C(l_n)$ along the entire inner slope, which yields an underestimation of l_n since in reality C will increase from $C(0)$ to $C(l_n)$.

Substitution of the values for q_T and β into equation (2.17) for the adaptation length l_a of the suspended load transport gives: $l_a = 1.8$ m at $t = 10$ s and at $t = 30$ s.
A friction coefficient $C \approx 0.025$ means a relatively extreme large bed shear (roughness factor k equals magnitude of water depth). This is in agreement with what was measured in the laboratory experiments of Visser (1988), see section 4.5.

Table 4.1 summarizes the main values for the various quantities and parameters. Table 4.1 contains also the value for the kinematic viscosity ν which is required for a number of transport formulae; this value is for a water temperature $T \approx 16°$C.

4.2.2 Schelde Flume experiment T5A

The sand-dike in this experiment was built up with dune-sand ($D_{10} = 0.15$ mm, $D_{50} = 0.22$ mm, $D_{90} = 0.29$ mm, mean sediment fall velocity for $T \approx 16°$C is $w_s = 0.028$ m/s). The cross-sectional dimensions have been identical to those of T3, with the exception of the inclination of the outer slope (1 : 4 at $t = t_0 = 0$ s in T5A, i.e. a dike profile, see Fig. 4.2). Also in this experiment the outer water level H_w was maintained as long as possible at $H_w = 0.75$ m by recirculating the discharge through the breach (q_T). The measured q_T is for $0 < t < 100$ s almost equal to that of T3: $q_T \approx 0.015$ (m^3/s)/m, see Steetzel and Visser (1992a, 1992b).

Also for this experiment, sediment transport computations have been done for $t = 10$ s and

$t = 30$ s ($\approx t_1$). Fig. 4.2 shows that at $t = 10$ s: $\beta \approx 20°$ and $L \approx 2.2$ m, and at $t = 30$ s: $\beta \approx 28°$ (along the adaptation length l_a) and $L \approx 2.2$ m. Sand transport calculations have also been done for $t = 100$ s, that is between t_1 en t_2, with a slope angle equal to the angle of repose ($\beta_1 = 32°$). Due to some water level decrease inside the flume at $t = 100$ s, caused by the discharge of an amount of water over 100 s of about $0.015 * 100\ m^3/m = 1.5\ m^3/m$ (the pumps started to recirculate water only after the water in the downstream section of the flume had raised to a certain level), the flow discharge at $t = 100$ s was somewhat lower than in the initial phase of the experiment, that is about $q_T \approx 0.010\ (m^3/s)/m$, see Steetzel and Visser (1992a).

Above values for the various quantities and parameters for the flow over the inner slope at $t = 10$ s, 30 s and 100 s, and the calculated values for d_c, u_c, $C(0)$, $\theta(0)$, $C(l_n)$, d_n, u_n, $\theta(l_n)$, l_n and l_a are shown in Table 4.1. Equation (2.17) predicts for $t = 10$ s a magnitude for the adaptation length of the sand transport ($l_a = 0.57$ m) being smaller than the magnitude of the adaptation length of the flow profile ($l_n = 0.72$ m) as given by (2.11). It is clear that the sand transport increases as the flow accelerates, at least as long as the sand concentration has not reached its maximum value. Consequently $l_a \geq l_n$, giving $l_a = 0.72$ m for $t = 10$ s.

In experiment T5A the level of the dike-top started to drop at $t_2 \approx 140$ s (see Fig. 4.2). Consequently the discharge over the top started to increase at t_2 (see Steetzel and Visser, 1992a, 1992b). At $t_2{}^+ = 240$ s ($t_2 < t_2{}^+ < t_3$), the values for H_w and Z_T were: $H_w \approx 0.72$ m and $Z_T \approx 0.50$ m. Substitution of these values into (2.1) gives: $q_T = 0.18\ (m^3/s)/m$, that is equal to the observed value (see Steetzel and Visser, 1992a).

The slope angle β strongly varied at $t_2{}^+$. Assuming β to be equal to $\beta_1 = 32°$ gives for $t_2{}^+$: $d_c = 0.15$ m, $C(l_n) = 0.032$, $d_n = 0.058$ m, $l_n = 2.6$ m and $l_a = 7.6$ m. At $t_2{}^+$ the length of the inner slope $L(t_2{}^+) \approx 1.0$ m, so $L(t_2{}^+) < l_n$ and $L(t_2{}^+) << l_a$. This means that at $t_2{}^+$ the water depth $d(L)$ at the toe of the slope was larger than the normal water depth d_n. An estimation of $d(L)$ follows from (2.13): $d(L) \approx 0.074$ m, so $u(L) \approx 2.4$ m/s and $\theta(L) \approx 15$ (see Table 4.1).

The fact that $L(t_2{}^+) << l_a$ means that the sand transport $s(L)$ at the toe of the inner slope was much smaller than the transport capacity at $t_2{}^+$, see equation (2.16).

4.2.3 Zwin'89 experiment

This field experiment was performed with local sand from the Zwin area. The D_{50} of this sand is equal to that of the dune-sand of experiment T5A: $D_{50} = 0.22$ mm. It is assumed that the values for D_{10} and D_{90} are also equal to those of the dune-sand: $D_{10} = 0.15$ mm, $D_{90} = 0.29$ mm).

The angle of inclination β of the inner slope at $t = t_0 = 0$ min ($\approx$ 12 h 49 min 30 s at 13 December 1989) was: $\beta_0 = 18°$. The cross-sectional dimensions of the sand-dike at $t = t_0$ have been: height of dike $H_d = 2.20$ m (above bottom of Zwin Channel, approximately at mean sea level), length of crown ≈ 7.5 m and inclination outer slope 1 : 1.25 (see Fig. 4.4).

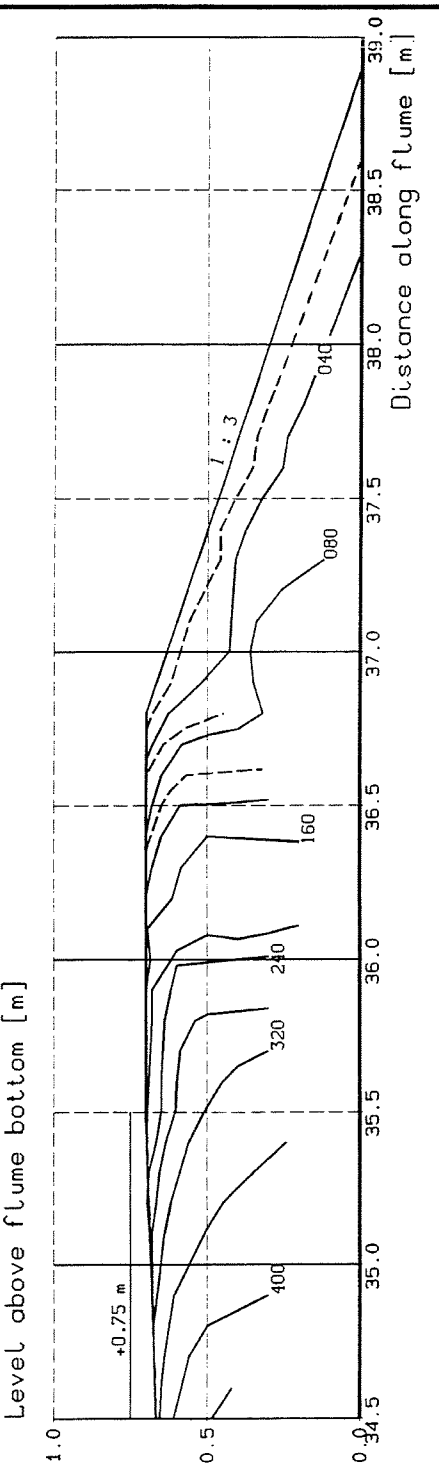

Times in seconds (t=0 at start of overflow)

DEVELOPMENT PROFILE OF SAND-DIKE IN EXPERIMENT T3

Test T3

DELFT HYDRAULICS

H1242-I

FIG. 4.1

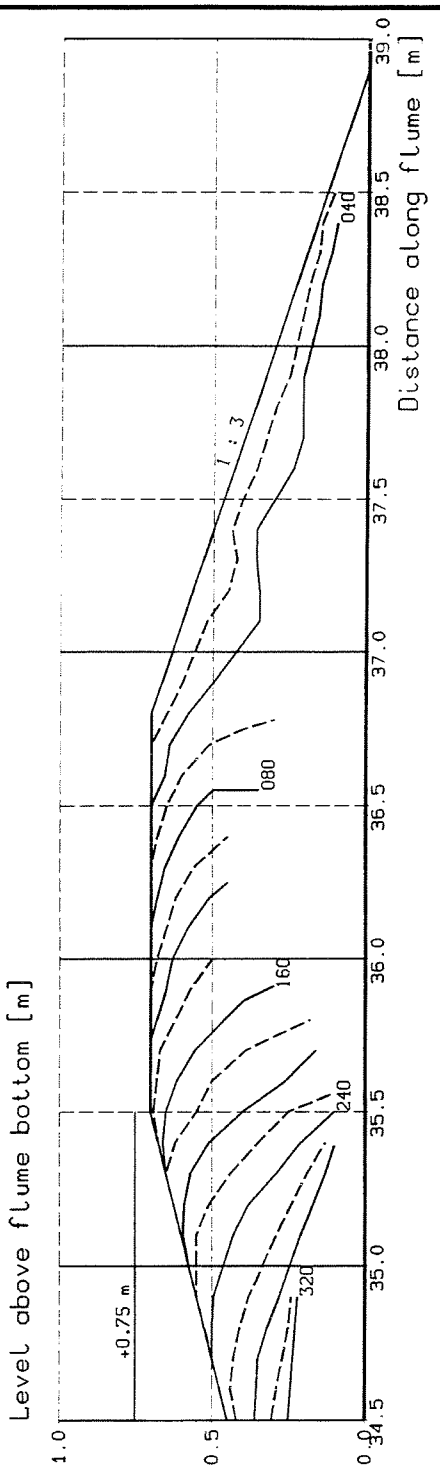

Times in seconds (t=0 at start of overflow)

DEVELOPMENT PROFILE OF SAND-DIKE IN EXPERIMENT T5A	Test T5A	
DELFT HYDRAULICS	H1242-I	FIG. 4.2

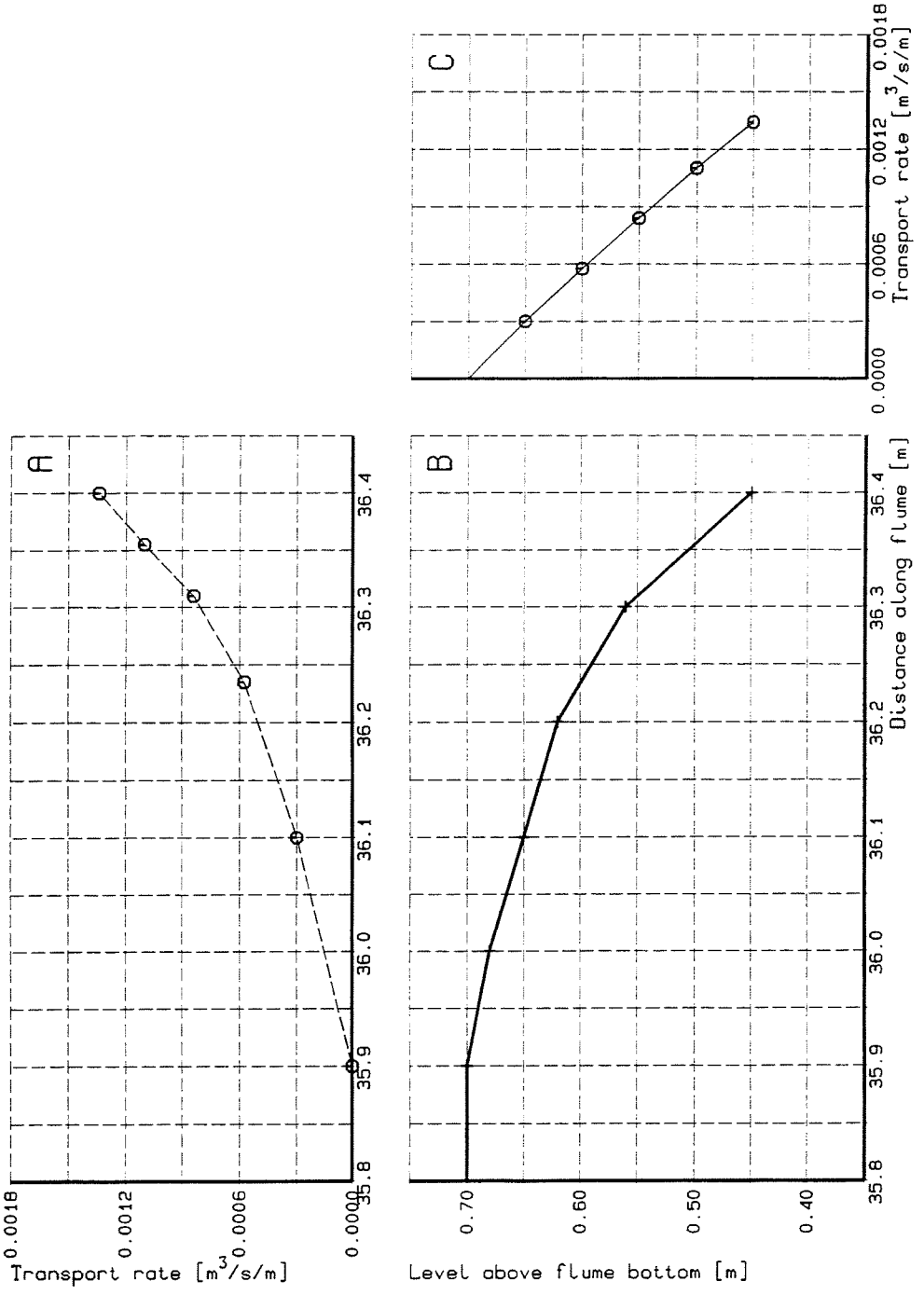

SAND TRANSPORT RATE ALONG INNER SLOPE AT t = 100 s IN EXP. T5A	Test T5A	
DELFT HYDRAULICS	H1242-I	FIG. 4.3

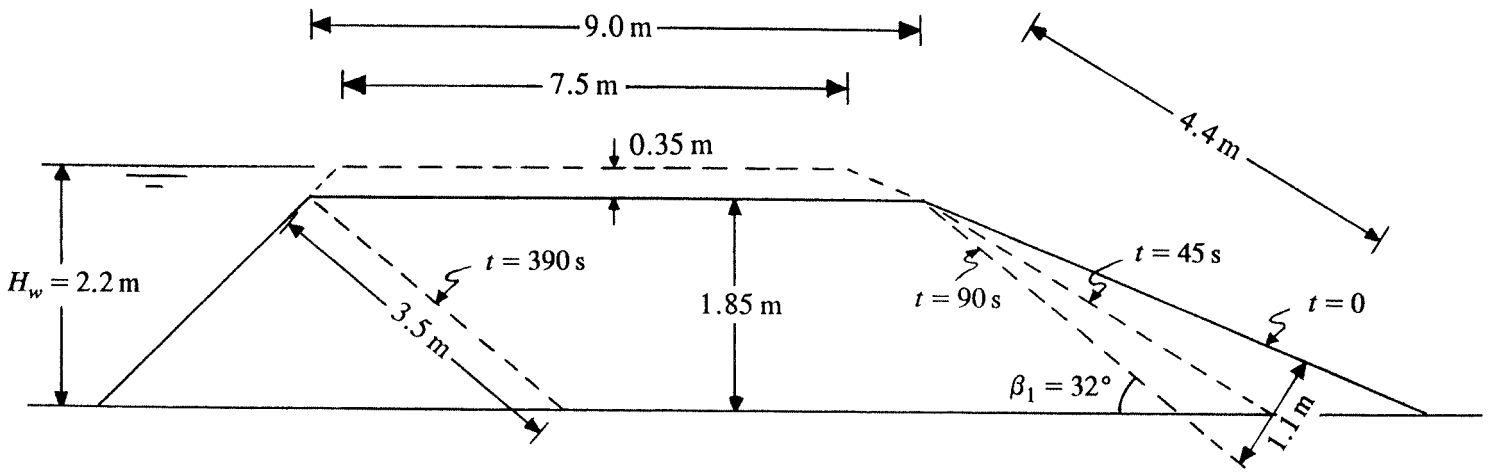

Fig. 4.4 Observed development of cross-section of sand-dam in Zwin'89 experiment.

The depth of the small pilot channel near the centre of the dike was at t_0: $H_d - Z_T \approx 0.35$ m.

The experiment was video-taped and photographed. The following values for t_1, t_2 and t_3 have been estimated from this visual material: $t_1 \approx 1.5$ min, $t_2 \approx 6.5$ min and $t_3 \approx 7.7$ min, see De Looff (1990). At $t = t_4 \approx 20$ min the flow turned from supercritical into subcritical, see Visser et al. (1990).

Sediment transport computations have been done for $t = 45$ s (just between t_0 and t_1, when $\beta \approx 25°$ and $L \approx 4.4$ m) and for $t = 240$ s (just between t_1 and t_2, when $\beta \approx \beta_1 = 32°$ and $L \approx 3.5$ m), see Table 4.1.

The water depth downstream in the pilot (initial) channel was between t_0 and t_1 (when $H_w \approx 2.0$ m) about 0.10 m. Substitution of $d_c \approx 0.10$ m into (2.2) gives: $q_T \approx 0.10$ (m^3/s)/m. Between t_1 and t_2, H_w raised from $H_w \approx 2.0$ m to $H_w \approx 2.1$ m, yielding an increase of the water depth downstream in the pilot channel from about 0.15 m to about 0.20 m. This means that at $t = 240$ s: $q_T \approx 0.25$ (m^3/s)/m.

Table 4.1 summarizes the main values for the various quantities and parameters. The friction coefficients calculated with (2.21) are relatively large, as in the case of the Schelde Flume experiments. This is roughly in agreement with what was measured in the field experiments described in section 3.1.3 (in which $C \approx 0.02$).

4.3 Determination of sediment transport in experiments

4.3.1 Schelde Flume experiment T3

Fig. 4.1 shows that experiment T3 supports the assumption behind equation (2.16), that the entrainment of sediment starts at $x = 0$. Since $u_*/w_s >> 1$ (see Table A.1 in Appendix A), the sediment transport along the slope can be written for $l_n \le x \le l_a$ as

$$s(x,t) \approx s_b(t) + \frac{x}{l_a} s_s(t) \qquad \text{for} \quad l_n \le x \le l_a \tag{4.1}$$

see chapter 2 (the time variable t has been added to stress the dynamic behaviour of the breach erosion process). At a distance l_n from the top of the inner slope ($x = 0$), the bed-load transport is equal to its equilibrium value and at $x = l_a$ the suspended load transport reaches its equilibrium value or transport capacity ($l_n = 0.67$ m and $l_a = 1.8$ m at $t = 10$ s, $l_n = 0.60$ m and $l_a = 1.8$ m at $t = 30$ s). For $x > l_a$ the sediment transport stays at its capacity, so theoretically it is constant.

Sediment transport rates (volumes of sand particles without voids), for instance at $t = 10$ s, have been determined from the profiles shown in Fig. 4.1 by estimating amounts of sand eroded between $t = 0$ s and $t = 20$ s along a length, from $x = 0$, of $l_n = 0.67$ m (for the test of the bed-load transport formulae) and along a length of $l_a = 1.8$ m (for the test of total load transport formulae), dividing the results by $\Delta t = 20$ s and multiply them by the factor $1 - p$

$= 0.6$ (the porosity p was measured in the Schelde Flume experiments as $p \approx 0.4$). The results are:

- at $x = l_n$: $s(0.67\,\text{m}, 10\,\text{s}) \approx 0.0011\,(\text{m}^3/\text{s})/\text{m}$, $s(0.60\,\text{m}, 30\,\text{s}) \approx 0.0020\,(\text{m}^3/\text{s})/\text{m}$,
- at $x = l_a$: $s(1.8\,\text{m}, 10\,\text{s}) \approx 0.0040\,(\text{m}^3/\text{s})/\text{m}$, $s(1.8\,\text{m}, 30\,\text{s}) \approx 0.0060\,(\text{m}^3/\text{s})/\text{m}$.

4.3.2 Schelde Flume experiment T5A

Fig. 4.2 shows the observed development of the cross-section of the sand-dike in experiment T5A. The adaptation lengths of the suspended load transport are $l_a \approx 0.72$ m at $t = 10$ s and $l_a \approx 0.61$ m at $t = 30$ s, both being much shorter than the length of the inner slope. The rates of sediment transport determined from Fig. 4.2 are:

- at $x = l_n$: $s(0.72\,\text{m}, 10\,\text{s}) \approx 0.0018\,(\text{m}^3/\text{s})/\text{m}$, $s(0.55\,\text{m}, 30\,\text{s}) \approx 0.0019\,(\text{m}^3/\text{s})/\text{m}$,
- at $x = l_a$: $s(0.72\,\text{m}, 10\,\text{s}) \approx 0.0018\,(\text{m}^3/\text{s})/\text{m}$, $s(0.61\,\text{m}, 30\,\text{s}) \approx 0.0020\,(\text{m}^3/\text{s})/\text{m}$.

In the first instance, there is no erosion for $x > l_a$ (see chapter 2), after some time resulting in the appearance of a bar for $x > l_a$, along which eventually a hydraulic jump is formed. Due to the turbulence generated in the hydraulic jump, the transport capacity firmly increases, resulting in the pick up and discharge of large amounts of sand downstream of $x = l_a$. Hydraulic jumps were also observed in Schelde Flume experiment T3 for $t > 40$ s (see profile inner slope at $t = 80$ s in Fig. 4.1). Due to the flow of water over the dike-crest, the water level decreased in the flume, leading to a decrease of q_T (see Steetzel and Visser, 1992a). According to equation (2.17), a smaller discharge rate q_T gives an adaptation length l_a smaller than the length of the inner slope, and thus as described above, a hydraulic jump.

The sand transport rates at time $t = 100$ s at $x = l_n = 0.38$ m and at $x = l_a = 0.42$ m have been estimated from Fig. 4.3 as:

- at $x = l_n$: $s(0.38\,\text{m}, 100\,\text{s}) \approx 0.0010\,(\text{m}^3/\text{s})/\text{m}$,
- at $x = l_a$: $s(0.42\,\text{m}, 100\,\text{s}) \approx 0.0012\,(\text{m}^3/\text{s})/\text{m}$.

The sediment transport rate at $t = 240$ s at $x = L \approx 1.0$ m (at the toe of the slope) has been estimated from Fig. 4.2 as:

- at $x = L$: $s(1.0\,\text{m}, 240\,\text{s}) \approx 0.0022\,(\text{m}^3/\text{s})/\text{m}$.

4.3.3 Zwin'89 experiment

Fig. 4.4 shows the observed development of the cross-section of the sand-dam in the Zwin'89 experiment (from photo- and video-recordings). Estimating sediment transport rates at $x = l_n = 2.1$ m and $x = L = 4.4$ m at time $t = 45$ s and at $x = l_n = 3.2$ m and $x = L = 3.50$ m at time $t = 240$ s from volumes eroded sand yields:

- at $x = l_n$: $s(2.1\,\text{m}, 45\,\text{s}) \approx (2.1/4.4)^2 * s(4.4\,\text{m}, 45\,\text{s}) \approx 0.0057\,(\text{m}^3/\text{s})/\text{m}$,
- at $x = l_n$: $s(3.2\,\text{m}, 240\,\text{s}) \approx (3.2/3.5) * s(3.5\,\text{m}, 240\,\text{s}) \approx 0.047\,(\text{m}^3/\text{s})/\text{m}$,
- at $x = L$: $s(4.4\,\text{m}, 45\,\text{s}) \approx [4.4\,\text{m} * (0.5 * 1.1\,\text{m}) * 0.6/0.65]/(90\,\text{s}) \approx 0.025\,(\text{m}^3/\text{s})/\text{m}$,
- at $x = L$: $s(3.5\,\text{m}, 240\,\text{s}) \approx [9.0\,\text{m} * 1.85\,\text{m} * 0.6/0.65]/(300\,\text{s}) \approx 0.051\,(\text{m}^3/\text{s})/\text{m}$.

The factor 0.6 represents the factor $1 - p$ (with a porosity $p = 0.4$ as in the Schelde Flume

experiments). The factor 1/0.65 represents an increase of sediment transport due to the growth of the breach in horizontal direction (see Visser, 1988).

4.4 Results sediment transport calculations

Sediment transport calculations have been done with the formulations of chapter 3 for the experimental conditions described in section 4.2. The formulations of Wilson (1966, 1987), Mizuyama (1977), Smart and Jaeggi (1983), Bathurst et al. (1987), Takahashi (1987) and Rickenmann (1991) apply to bed-load transport. In the first instance, the equilibrium values for the sand transport rates (s_b) predicted by these formulae have been compared with the experimental rates at $x = l_n$.

The formulations of Engelund and Hansen (1967), Yang (1979), Mastbergen and Winterwerp (1987) and Takahashi (1991) apply to total sediment transport, conceived here as suspended load transport with adaptation length l_a. The remaining formulae apply to total sediment transport consisting of bed-load transport and suspended load transport, in which for the situations under consideration $s_b << s_s$ since $u_*/w_s >> 1$ (see also Table A.10). The equilibrium values for the sediment transport rates (s_t) given by all these formulae have been compared with the experimental rates at $x = l_a$.

Equilibrium values for the sand transport and local rates of sand transport have been computed as volume transported sediment (sediment without voids). In cases where the transport formulae predict very or infinitely large transport rates, it has been assumed that $c(x) \leq 0.6$, which means with (2.19) that

$$s(x) \leq 1.5\, q_T \tag{4.2}$$

In cases where $L > l_a$ (or $L > l_n$), the equilibrium value $s_t = s(l_a)$ (or $s_b = s(l_n)$) for the sediment transport has been computed. In cases where $L < l_a$, the sediment transport $s(L)$ at the toe of the inner slope has been calculated as

$$s(L,t) = s_b(t) + \frac{L}{l_a}\, s_s(t) \tag{4.3}$$

(when also $L < l_n$, as in Schelde Flume experiment T5A at $t = 240$ s, then apparent equilibrium transport rates $s_b(L)$ and $s_s(L)$ have been computed using the local flow conditions at $x = L$, see Table 4.1).

The computational results are shown in Tables A.1 through A.15 in Appendix A. The calculations and the results are briefly elucidated below.

4.4.1 Wilson (1966)

The rates of sand transport calculated with (3.1) are 3.1 to 8.8 times larger than the experimental values.

4.4.2 Wilson (1987)

For large values of θ as in the present situation, Wilson's (1987) formula (3.3) predicts nearly the same sediment transport rates as Wilson's (1966) formula (3.1). The sensitivity of both formulae to a variation in particle diameter D is very small.

4.4.3 Mastbergen and Winterwerp (1987)

Computations with the friction coefficients of Table 4.1 and with $C = 0.0125$ (as proposed by Mastbergen and Winterwerp, 1987) have been done; the results are given in Table A.3.1 and Table A.3.2, respectively. Mastbergen and Winterwerp's (1987) formula significantly overestimates the present sediment transport rates, especially for slope angles β close to the angle of repose ϕ. For $\beta = 32°$ the formula predicts infinitely large transport rates, i.e. a situation of auto-suspension.

The sensitivity of the erosion rate E to the value of D is relatively small, see equation (3.5). In the present eight cases this also holds for $E - S_c$.

4.4.4 Mizuyama (1977)

This formula gives negative results for $\beta > 14°$; consequently, application to the present eight cases is not possible.

4.4.5 Smart and Jaeggi (1983)

$(D_{90}/D_{30})^{0.2} \approx 1.1$, both for the sand in experiment T3 and for the sand in experiment T5A. It is assumed that the sand in the Zwin'89 experiment had the same value for this ratio. Formula (3.11) predicts sand transport rates that are 4.2 to 12 times the experimental rates. The sensitivity of the formula to the particle diameter D is very small.

4.4.6 Bathurst, Graf and Cao (1987)

The D_{16} of the sand in experiment T3 is about 0.074 mm, that of the sand in experiment T5A about 0.16 mm. It is assumed that the sand in the Zwin'89 experiment had also a D_{16} of about 0.16 mm This means with (3.14) that q_{cr} is very small compared to q_T, so that according to (3.13) the transport s_b is independent of the particle diameter D.

Formula (3.13) overestimates the experimental sand transport rates by a factor ranging between 1.7 and 38.

4.4.7 Takahashi (1987)

For $\beta > 14°$ equation (3.9) gives negative values for ξ^2. For these cases it has been assumed that $\xi^2 = 0$. Then (3.16) and (3.17) give unrealistic small values for the friction coefficients C (see Table A.7). However, this is not the cause that (3.15) predicts sand transport rates that are 5.2 to 123 times the measured rates, because the sensitivity of (3.15) to C is very small (see section 4.5). This also holds with respect to the particle diameter D.

4.4.8 Rickenmann (1991)

The calculated sand transport rates are 6.7 to 123 times the observed rates. The sensitivity of this formula to the particle diameter D is very small.

4.4.9 Engelund and Hansen (1967)

Formula (3.23) predicts sand transport rates that are 3.7 to 9.5 times the measured rates. The sensitivity of this formula to a variation of D is such that s_t is proportional to D^{-1} (apart from roughness effects).

4.4.10 Van Rijn (1984a, 1984c)

Formulae (3.25) and (3.26) show that, according to Van Rijn (1984a, 1984c), the bed-load transport increases relatively strongly with D. The reason behind this is that the thickness of the bed-load transport layer increases both with D and the parameter T of equation (3.27), see Van Rijn (1984a). The suspended load transport decreases with D, as also the total load transport (see Table A.10).

Optimal results have been obtained with $a = 3D_{90}$, see (3.33). Equation (3.34) predicts values for the sand concentration c_a at this distance a above the bed between 0.83 (T3, $t = 10$ s) and 7.0 (Zwin'89 experiment, $t = 240$ s). These high values for c_a are not realistic; the maximum value of c_a is about 0.6, i.e. $c_a \leq 0.6$.

The agreement between calculated and observed transport rates is reasonable. An exception is the transport rate at $t = 240$ s in the Zwin'89 experiment, that is underestimated by Van Rijn's formulae with a factor 0.3.

4.4.11 Bagnold (1963, 1966)

Bagnold's formula (3.36) predicts auto-suspension (infinite transport rates) in all situations, which is not in agreement with the observations.

4.4.12 Yang (1979)

Formula (3.37) predicts values for the depth-averaged concentration c_t being larger than 0.51, resulting in unrealistic large sand transport rates.

4.4.13 Bagnold-Bailard (1981)

The agreement between the predictions by (3.39) and the experimental values is reasonable, except for the sand transport rate in the Zwin'89 experiment at $t = 240$ s: equation (3.39) predicts here a situation close to auto-suspension (due to a large value of β). Formula (3.39) is very sensitive to a variation in D: the transport rate strongly decreases with an increasing D.

4.4.14 Bagnold-Visser (1988)

The agreement between calculated and experimental values is rather good. The sensitivity of this formula to a variation in the particle diameter D is rather large but somewhat less than that of Bagnold-Bailard's (1981) formula.

4.4.15 Takahashi (1991)

This formula predicts for all cases sediment transport rates larger than $1.5\,q_T$.

4.5 Discussion

Wilson's formula (3.1) gives similar results as Wilson's (3.3), Mizuyama's (3.8) gives no results at all. Table A.16 summarizes the sediment transport rates as computed with the remaining formulae (given in Tables A.2 through A.3.2 and A.5 through A.15). The table also includes the experimental sand transport rates. Table A.17 presents the values of the ratio ζ between calculated and experimental sand transport rates (the unrealistic large values for this ratio resulting from the application of the formulae of Bagnold (1963, 1966), Yang (1979) and Takahashi (1977) have not been included). Table A.17 clearly indicates that most of the sediment transport formulae overestimate the experimental sand transport rates considerably.

A parameter r is defined such that $r = \zeta$ if $\zeta \geq 1$ and $r = 1/\zeta$ if $\zeta < 1$. Averaging r over the eight cases yields a mean value $\bar{r}$ that is a measure for this agreement. From Table A.17 the following list of the five formulae with the lowest values for $\bar{r}$ can be made up:

1. Bagnold-Visser (1988), $\bar{r} = 1.3$
2. Van Rijn (1984a, 1984c), $\bar{r} = 1.6$
3. Bagnold-Bailard (1981), $\bar{r} = 2.2$
4. Wilson (1987), $\bar{r} = 4.9$
5. Engelund and Hansen (1967), $\bar{r} = 6.4$

The formulae of Bagnold-Visser (1988) and Van Rijn (1984a, 1984c) predict the experimental values within a factor 2. The Bagnold-Visser formula is the only one doing that also in all individual cases. This conclusion and the above list apply to the sand transport in

phases I, II and III of the five-step breach erosion process as described in chapter 2, for which $Fr > 1$ (in fact the test has been done here for $2.8 \leq Fr \leq 4.1$) and in which suspended load transport dominates bed-load transport. Further it has been assumed that:

- the suspended load transport has an adaptation length l_a that is described by (2.17);
- the bar that will be formed after some time at $x > l_a$ if $L > l_a$ will be eroded and removed due to a higher turbulence intensity;
- the friction coefficient is given by (2.21) with (2.22) and (2.23).

The following remarks are made about the sensitivity of above conclusion to the various assumptions.

A. It has been assumed that suspended load transport has an adaptation length l_a and that the adaptation length of bed-load transport is relatively small, so that at $x = l_n$ the bed-load transport is approximately equal to its equilibrium value. The application of this assumption to the bed-load formulae of Wilson (1966, 1987), Smart and Jaeggi (1983), Bathurst et al. (1987), Takahashi (1987) and Rickenmann (1991) has implied that the sand transport rates given by these formulae have been compared with the experimental rates at $x = l_n$ and not with the larger rates at $x = l_a$. As described before, the relatively large values of the mobility parameter θ in the present experiments indicate that the sediment transport is not restricted to a layer immediately above the bed with a thickness of a few particle diameters. Instead, in the first phases of the breach erosion process the sediment particles are transported in a dense layer above the bed, supported by grain-grain interaction, with a thickness of about half the water depth (see section 3.1.1). This sheet flow has an adaptation length much larger than that of bed-load transport. Applying the above bed-load transport formulae, it is therefore further assumed that the sand transport has an adaptation length l_a, except Van Rijn's (1984a, 1984c) bed-load transport. This assumption significantly improves the performance of the 'bed-load formulae' (3.3) of Wilson, (3.11) of Smart and Jaeggi, (3.13) of Bathurst et al., (3.15) of Takahashi and (3.20) of Rickenmann (see Table A.18) in the present application. The list of best performing formulae becomes now: 1. Bagnold-Visser ($\bar{r} = 1.3$), 2. Van Rijn ($\bar{r} = 1.6$), 3. Bagnold-Bailard ($\bar{r} = 2.2$), 4. Bathurst et al. ($\bar{r} = 2.3$) and 5. Wilson ($\bar{r} = 2.5$).

B. Suppose that the prediction of the friction coefficient by (2.21) with (2.22) and (2.23) is not correct and that $C = 0.058$ (i.e. a Chézy coefficient $C_h = g/C^2 = 13\ \mathrm{m}^{0.5}/\mathrm{s}$, as measured by Visser (1988) in experiments comparable to the Schelde Flume experiments) and for larger depths that $C = 0.0157$ (i.e. a Chézy coefficient of $25\ \mathrm{m}^{0.5}/\mathrm{s}$, as measured in the field experiments in the Slaak Estuary, see section 4.2.3). The resulting values for the ratio ζ are given in Table A.19. The list reads now: 1. Bagnold-Visser ($\bar{r} = 1.3$), 2. Van Rijn ($\bar{r} = 1.7$), 3. Bagnold-Bailard ($\bar{r} = 2.2$), 4. Bathurst et al. ($\bar{r} = 2.3$) and 5. Wilson ($\bar{r} = 3.3$). The relation between sediment transport capacity and friction coefficient C varies rather strongly in the various transport formulae:

$s_t \sim C^{5/6}$: Takahashi (1991)

$s_b \sim C^{1/2}$: Wilson (1966, 1987), Mizuyama (1977)

$s_b \sim C^{1/6}$: Mastbergen and Winterwerp (1987)

$s_b \sim 1$: Smart and Jaeggi (1983), Bathurst et al. (1987), Takahashi (1987), Rickenmann (1991), Bagnold's (1963, 1966) bed-load transport

$s_b \sim C^{-1/6}$: Engelund and Hansen (1967)

$s_b \sim C^{-1/3}$: Bagnold's (1963, 1966) suspended load transport (for $w_s/u >> \tan\beta$), Bagnold-Bailard's (1981) suspended load transport (for $w_s/u >> 0.01\tan\beta$), Bagnold-Visser's (1988) suspended load transport

$s_t, s_s \sim C^{-1/2}$: Yang (1979), Van Rijn's (1984a, 1984c) suspended load transport

$s_b \sim C^{-1}$: Van Rijn's (1984a, 1984c) bed-load transport

The above relations between s_b, s_s or s_t on the one side and C on the other side follow from the substitution of (2.4) into the various transport formulations, giving equations for the equilibrium values of the sand transport rates as function of the parameters q, β, D (or w_s) and C. Especially s_b in the formulae of Takahashi (1991), Wilson (1966, 1987), Mizuyama (1977), Yang (1979) and s_b and s_s in the formulae of Van Rijn (1984a, 1984c) are sensitive to variations of C. To a lesser extent this also applies to the formulae for the suspended load transport of Bagnold (1963, 1966), Bagnold-Bailard (1981) and Bagnold-Visser (1988).

C. With its coefficient equal to the unity equation (2.17) gives an order of magnitude for l_a. According to Galapatti the coefficient is somewhat less, i.e. about 0.5. Consequently also sand transport calculations and comparisons with the experimental results have been done with l_a given by

$$l_a \approx 0.5 \frac{q_T}{w_s \cos\beta} \tag{4.4}$$

(but $l_a \geq l_n$). The resulting values for ζ are shown in Table A.20. The list becomes in this situation: 1. Van Rijn ($\bar{r} = 1.6$), 2. Bagnold-Visser ($\bar{r} = 2.0$), 3. Bathurst et al. ($\bar{r} = 3.3$), 4. Wilson ($\bar{r} = 3.5$), 5. Bagnold-Bailard ($\bar{r} = 3.7$). The application of (4.4) instead of (2.17) gives generally worse results. Only Van Rijn's formulation gives equal results with (4.4) and (2.17).

D. Finally computational and experimental sand transport rates have been determined assuming that l_a is described by

$$l_a \approx 2 \frac{q_T}{w_s \cos\beta} \tag{4.5}$$

The resulting values for the ratio ζ have been given in Table A.21. The list reads now: 1. Bagnold-Bailard ($\bar{r} = 1.6$), 2. Bagnold-Visser ($\bar{r} = 1.9$), 3. Bathurst et al. ($\bar{r} = 2.2$), 5. Wilson ($\bar{r} = 2.2$), Smart and Jaeggi ($\bar{r} = 2.3$). Most transport formulae perform better with (4.5) compared with (2.17). Only the formulae of Bagnold-Visser and Van Rijn give worse results with (4.5) than with (2.17).

It is concluded from the present tests that the overall best results have been obtained with the Bagnold-Visser (1988) formula (3.41) and equation (2.17) for the adaptation length l_a. This conclusion is not very sensitive to a variation of the bed friction coefficient C, i.e. to the assumptions made about this coefficient.

5 Conclusions and recommendations

The process of entrainment of sand from, and transport over, a relatively steep slope, as taking place in the first three phases of the development of a breach in a sand-dike, is very exceptional from a hydraulic point of view:

- The mobility parameter θ varies between about 0.3 at the top of the inner slope and about 10 to 100 (or more) at $x \geq l_n$ along the slope (see Table 4.1).
- The Froude number Fr increases along this slope from $Fr = 1$ at the top to substantially larger values at $x \geq l_n$ or at $x = L$ (here: $2.8 \leq Fr \leq 4.1$, see Table A.1).
- The angle of inclination attains values of $\beta \approx 32°$ and larger.
- The roughness factor k in the equations (2.21) through (2.23) increases from $3D_{90}$ at the top of the slope to values having the order of magnitude of the water depth at $x \geq l_n$.
- The depth-averaged sand concentration gets values up to $c \approx 0.25$.

None of the present sediment transport formulae have been set-up for and tested to such extreme conditions. The validity ranges of the formulae (if known) are well exceeded in the present tests, especially those of the mobility parameter θ, the slope angle β and (to a lesser extent for some formulae) the depth-averaged concentration c.

Most of the tested sediment transport formulae predict transport rates much larger than the experimental rates. Only the Bagnold-Visser formula, see Visser (1988), predicts sand transport rates within a factor two of the experimental values. With the formulation of Van Rijn (1984a, 1984c) this is possible within a factor three. All other formulae give larger deviations from the experimental data.

These conclusions hold for the phases I, II en III of the breach erosion process (see chapter 2), when the flow is supercritical. The good performance of the Bagnold-Visser formula confirms the good results obtained before, see Visser (1988, 1994). Again it is emphasized that the formula has not been derived for a situation where the entrainment of sediment is so large. This applies to both the theory behind it and the empirical test of the efficiency factor.

Due to the large sand entrainment the flow rate of the sand-water mixture increases substantially along the inner slope and the sand concentration becomes very large (so that the effect of hindered entrainment is possibly not negligible). In fact further study is necessary to investigate the effects of the large rate of sediment entrainment on the breach erosion process. For the time being it is recommended to apply the formula of Bagnold-Visser in a mathematical breach growth model for the description of the first phases (i.e. as long as the flow is super critical) of the breach erosion process.

The present study does not recommend a formulation for the important phases IV (when $Fr \geq 1$) and V (when $Fr < 1$), in which the bulk of the breach erosion takes place and also the dimensions of the final breach are determined. Only recently the experimental data

required have (partly) become available for that, see Visser et al. (1995). Consequently above conclusions do not fit these phases. Voogt et al. (1991) tested the formulae of Engelund and Hansen (1967) and Van Rijn (1984a, 1984c) for relatively large flow velocities in subcritical flow. They concluded that also in these circumstances both formulae give good agreements with the experimental data. So it might be that these formulae can be applied in the later phases of the breach erosion process. Tests of these formulae and of the Bagnold-Visser (1988) formula to experimental data are recommended.

Acknowledgements

The investigation described in this report was financially supported by the Technical Advisory Committee on Water Retaining Structures (TAW) of the Ministry of Transport, Public Works and Water Management in the Netherlands. The author wishes to thank W.Th. Bakker, J. van de Graaff, A.W. Kraak and H.J. Steetzel for their comments and stimulating support during the investigation and preparation of this report. The author also wishes to thank J.A. Battjes for his critical review of the final manuscript.

References

Allen, J.R.L., 1982. *Developments in sedimentology: sediment structures, their character and physical basis*, vol. 1. Elsevier Scientific Publication Co, Amsterdam, The Netherlands.

Ashida, K., Takahashi, T. and Mizuyama, T., 1978. Study of bed load equations for mountain streams. *Shin-sabo*, vol. 30, no. 4, pp. 9-17 (in Japanese).

Bagnold, R.A., 1963. Mechanics of marine sedimentation. In *The Sea: Ideas and observations*, vol. 3. Interscience, New York, USA, pp. 507-528.

Bagnold, R.A., 1966. An approach to the sediment transport problem from general physics. *Geological Survey Professional Paper* 422-I, U.S. Government Printing Office, Washington, D.C., USA.

Bailard, J.A., 1981. An energetics total load sediment transport model for a plane sloping beach. *J. Geophysical Res.*, vol. 86, C11, pp. 10938-10954.

Bathurst, J.C., Graf, W.H. and Cao, H.H., 1987. Bed load discharge equations for steep mountain rivers. In *Sediment Transport in Gravel-Bed Rivers*, Thorne, Bathurst and Hey (eds.), John Wiley & Sons, Chichester, Great Britain, pp. 453-477.

De Looff, A.P., 1990. Bresgroei in een zanddijk, feitenverslag van een proef (Breach growth in a sand-dike, report of a field experiment. *Rep. WBA-R-90.041*, Dienst Weg- en Waterbouwkunde, Rijkswaterstaat, Ministry of Transport, Public Works and Water Management, Delft, The Netherlands.

Engelund, F., 1970. Instability of erodible beds. *J. Fluid Mech.*, vol. 42, pp. 225-244.

Engelund, F. and Hansen, E., 1967. *A monograph on sediment transport.* Technisk Forlag, Copenhagen, Denmark.

Galappatti, R., 1983. A depth-integrated model for suspended transport. *Communications on Hydraulics*, Rep. no. 83-7, Dept. Civil Eng., Delft Univ. Techn, Delft, The Netherlands.

Galappatti, R. and Vreugdenhil, C.B., 1985. A depth-integrated model for suspended sediment transport. *J. Hydraulic Res.*, IAHR, vol. 23, pp. 359-377.

Guy, H.P., Simons, D.B. and Richardson, E.V., 1966. Summary of alluvial channel data from flume experiments, 1956-1961. *U.S. Geological Survey Professional Paper* 462-I, Washington, D.C., USA.

Jaeggi, M.N.R. and Rickenmann, D., 1987. Application of sediment transport formulae in mountain streams. *Proc. 22nd Congress IAHR*, Lausanne, Switserland, pp. A98-103.

Kennedy, J.F., 1969. The formation of sediment ripples, dunes and anti-dunes. *Ann. Rev. Fluid Mech.*, vol. 1, pp. 147-168.

Kraak, A.W., Bakker, W.T, Van de Graaff, J., Steetzel, H.J. and Visser, P.J., 1994. Breach-growth research programme and its place in damage assessment for a polder. *Proc. 24th Int. Conf. Coastal Eng.*, Kobe, Japan, pp. 2197-2206.

Mastbergen, D.R. and Winterwerp, J.C., 1987. Het gedrag van zand-watermengselstromingen boven water; verslag experimentele vervolgstudie (The behaviour of sand-water mixture flows above the water level). Delft Hydraulics, *Rep. Z46-02*, Delft, The Netherlands.

Meyer-Peter, E. and Müller, R., 1948. Formulas for bed-load transport. *Proc. 2nd Congress IAHR*, Appendix 2, pp. 39-64, Stockholm, Sweden.

Mizuyama, T., 1977. Bed load transport in steep channels. Ph.D thesis, Kyoto Univ., Kyoto, Japan (in Japanese).

Peterson, A.W. and Howells, R.F., 1973. A compendium of solids transport data for mobile boundary channels. *Rep. no. HY-1973-ST3*, Dept. Civil Eng., Univ. of Alberta, Canada.

Rickenmann, D., 1991. Hyperconcentrated flow and sediment transport at steep slopes. *J. Hydr.* Eng., ASCE, vol. 117, pp. 1419-1439.

Schoklitsch, A., 1962. *Handbuch des Wasserbaues*, 3rd edition, Springer-Verlag, Vienna, Austria.

Shields, A., 1936. Anwendung der Aehnlichkeitsmechanik und der Turbulenzforschung auf die Geschiebebewegung. *Mitt. der Preuss. Versuchsanstalt für Wasserbau und Schiffbau*, Heft 26, Berlin, Germany.

Shook, C.A., Gillies, R., Haas, D.B., Husband, W.H.W. and Small, M. 1982. Flow of coarse and fine sand slurries in pipelines. *J. Pipelines*, Elsevier, vol. 3, pp. 13-21.

Sieben, A., 1993. Hydraulics and morphology of mountain rivers: a literature survey. *Communications on hydraulic and geotechnical engineering*, Rep. no. 93-4, Fac. Civil Eng., Delft Univ. Techn., Delft, The Netherlands.

Smart, G.M. and Jaeggi, M., 1983. Sediment transport on steep slopes. *Mitteilungen der Versuchsanhalt für Wasserbau, Hydrologie und Glaziologie*, No. 64, Eidgenossischen Technischen Hochschule, Zurich, Switserland.

Smart, G.M., 1984. Sediment transport formula for steep channels. *J. Hydr. Eng.*, ASCE, vol. 110, pp. 267-276.

Steetzel, H.J. and Visser, P.J., 1992a. Bresgroei, Deel II: 2DV-ontwikkeling initiële bres; Band A: Verslag modelonderzoek Scheldegoot (Breach growth, Part II: 2DV-development initial breach: Report experiments in Schelde Flume). *Rep. H1242-IIA*, Delft HydraulicsDelft Univ. Techn., Delft, The Netherlands.

Steetzel, H.J. and Visser, P.J., 1992b. Profile development of dunes due to overflow. *Proc. 23rd Int. Conf. Coastal Eng.*, Venice, Italy, pp. 2669-2679.

Takahashi, T., 1978. Mechanical characteristics of debris flow. *J. Hydr. Div.*, ASCE, vol. 104, pp. 1153-1169.

Takahashi, T., 1980. Debris flow on prismatic open channel. *J. Hydr. Div.*, ASCE, vol. 106, pp. 381-396.

Takahashi, T., 1987. High velocity flow in steep erodible channels. *Proc. 22nd Congress IAHR*, Lausanne, Switserland, pp. A42-53.

Takahashi, T., 1991. *Debris flow.* IAHR monograph, Balkema, Rotterdam, 165 pp.

Van Rijn, L.C., 1984a. Sediment transport, Part I: bed load transport. *J. Hydr. Eng.*, ASCE, vol. 110, pp. 1431-1456.

Van Rijn, L.C., 1984b. Sediment pick-up functions. *J. Hydr. Eng.*, ASCE, vol. 110, pp. 1494-1502.

Van Rijn, L.C., 1984c. Sediment transport, Part II: suspended load transport. *J. Hydr. Eng.*, ASCE, vol. 110, pp. 1613-1641.

Van Rijn, L.C., 1985. Sand transport at high velocities; report on experimental research. Delft Hydraulics, *Rep. M2127* parts A and B, Delft, The Netherlands.

Van Rijn, L.C., 1993. *Principles of sediment transport in rivers, estuaries and coastal seas.* Aqua Publications, Amsterdam, The Netherlands.

Visser, P.J., 1988. A model for breach growth in a dike-burst. *Proc. 21st Int. Conf. Coastal Eng.*, Malaga, Spain, pp. 1897-1910.

Visser, P.J., 1994. A model for breach growth in sand-dikes. *Proc. 24th Int. Conf. Coastal Eng.*, Kobe, Japan, pp. 2755-2769.

Visser, P.J., Ribberink, J.S. and Kalkwijk, J.P.Th., 1986. Ontwikkeling stroomgat en debiet bij dijkdoorbraak; deelstudie voor een pompaccumulatiecentrale (Development of the breach and flow discharge in a dike-burst. *Rep. no. 8-86*, Hydraulic and Geotechnical Eng. Div., Dept. Civ. Eng., Delft Univ. Techn., Delft, The Netherlands.

Visser, P.J., Vrijling, J.K. and Verhagen, H.J., 1990. A field experiment on breach growth in sand-dikes. *Proc. 22nd Int. Conf. Coastal Eng.*, Delft, pp. 2087-2100.

Visser, P.J., Kraak, A.W., Bakker, W.T., Smit, M.J., Snip, D.W., Steetzel, H.J. and Van de Graaff, J., 1995. A large-scale experiment on breaching in sand-dikes. *Proc. Coastal Dynamics'95*, Gdansk, Poland.

Voogt, L., Van Rijn, L.C. and Van den Berg, J.H., 1991. Sediment transport of fine sands at high velocities. *J. Hydr. Eng.*, ASCE, vol. 117, pp. 869-890.

Wilson, K.C., 1966. Bed-load transport at high shear stress. *J. Hydr. Div.*, ASCE, vol. 92, pp. 49-59.

Wilson, K.C., 1987. Analysis of bed-load motion at high shear stress. *J. Hydr. Eng.*, ASCE, vol. 113, pp. 97-103.

Wilson, K.C., 1989. Mobile-bed friction at high shear stress. *J. Hydr. Eng.*, ASCE, vol. 115, pp. 825-830.

Wilson, K.C and Nnadi, F.N., 1992. Motion of mobile beds at high shear stress. *Proc. 23rd Int. Conf. Coastal Eng.*, Venice, Italy, pp. 2917-2925.

Wilson, K.C., 1992. Personal communication.

Winterwerp, J.C., De Groot, M.B., Mastbergen, D.R. and Verwoert, H., 1990. Hyper-concentrated sand-water mixture flows over flat bed. *J. Hydr. Eng.*, ASCE, vol. 116, pp. 36-54.

Winterwerp, J.C., Bakker, W.T., Mastbergen, D.R. and Van Rossum, H., 1992. Hyper-concentrated sand-water mixture flows over erodible bed. *J. Hydr. Eng.*, ASCE, vol. 118, pp. 1508-1525.

Yang, C.T., 1979. Unit stream power equations for total load. *J. Hydrology*, vol. 40, pp. 123-138.

Yang, C.T. and Kong, X., 1991. Energy dissipation rate and sediment transport. *J. Hydr. Res.*, IAHR, vol. 29, pp. 457-474.

Appendix A Tables A.1 through A.21

		Schelde Flume experiments						Zwin'89 exp.	
D_{50}	[mm]	0.10		0.22				0.22	
t	[s]	10	30	10	30	100	240	45	240
β	[°]	20	23	20	28	32	32	25	32
q_T	[(m^3/s)/m]	0.015	0.015	0.015	0.015	0.010	0.18	0.10	0.25
C	[-]	0.025	0.027	0.022	0.028	0.032	0.0089	0.026	0.032
u	[m/s]	1.3	1.3	1.3	1.3	1.2	2.4	2.5	3.5
d	[m]	0.012	0.012	0.011	0.011	0.0085	0.074	0.040	0.072
Fr	[-]	3.7	3.8	3.9	4.1	4.1	2.8	4.0	4.1
$u_\star/w_s$	[-]	22	24	7.0	8.1	7.5	8.2	17	26
θ	[-]	24	28	11	14	12	15	46	106
l_n	[m]	0.67	0.60	0.72	0.55	0.38	2.6	2.1	3.2
l_a	[m]	1.8	1.8	0.72	0.61	0.42	7.6	4.6	12
L	[m]	2.0	1.9	2.2	2.2	1.3	1.0	4.4	3.5
$s_b(l_n)$	[(m^3/s)/m]	0.0059	0.0071	0.0056	0.0087	0.0069		0.050	0.17
$s_b(L)$	[(m^3/s)/m]						0.0090		
$c(l_n)$	[-]	0.28	0.32	0.27	0.37	0.41		0.33	0.41
$c(L)$	[-]						0.047		

Table A.1 Applicaton of Wilson (1966) to the Schelde Flume experiments T3 ($D_{50} = 0.10$ mm) and T5A ($D_{50} = 0.22$ mm) and the Zwin'89 experiment.

		Schelde Flume experiments						Zwin'89 exp.	
D_{50}	[mm]	0.10		0.22				0.22	
t	[s]	10	30	10	30	100	240	45	240
β	[°]	20	23	20	28	32	32	25	32
q_T	[(m^3/s)/m]	0.015	0.015	0.015	0.015	0.010	0.18	0.10	0.25
C	[-]	0.025	0.027	0.022	0.028	0.032	0.0089	0.026	0.032
u	[m/s]	1.3	1.3	1.3	1.3	1.2	2.4	2.5	3.5
d	[m]	0.012	0.012	0.011	0.011	0.0085	0.074	0.040	0.072
Fr	[-]	3.7	3.8	3.9	4.1	4.1	2.8	4.0	4.1
θ	[-]	24	28	11	14	12	15	46	106
l_n	[m]	0.67	0.60	0.72	0.55	0.38	2.6	2.1	3.2
l_a	[m]	1.8	1.8	0.72	0.61	0.42	7.6	4.6	12
L	[m]	2.0	1.9	2.2	2.2	1.3	1.0	4.4	3.5
$s_b(l_n)$	[(m^3/s)/m]	0.0058	0.0069	0.0055	0.0085	0.0067		0.049	0.17
$s_b(L)$	[(m^3/s)/m]						0.0087		
$c(l_n)$	[-]	0.28	0.32	0.27	0.36	0.40		0.33	0.40
$c(L)$	[-]						0.046		

Table A.2 Application of Wilson (1987) to the Schelde Flume experiments T3 ($D_{50} = 0.10$ mm) and T5A ($D_{50} = 0.22$ mm) and the Zwin'89 experiment.

	Schelde Flume experiments						Zwin'89 exp.	
D_{50} [mm]	0.10		0.22				0.22	
t [s]	10	30	10	30	100	240	45	240
β [°]	20	23	20	28	32	32	25	32
q_T [(m^3/s)/m]	0.015	0.015	0.015	0.015	0.010	0.18	0.10	0.25
C [-]	0.025	0.027	0.022	0.028	0.032	0.0089	0.026	0.032
u [m/s]	1.3	1.3	1.3	1.3	1.2	2.4	2.5	3.5
d [m]	0.012	0.012	0.011	0.011	0.0085	0.074	0.040	0.072
Fr [-]	3.7	3.8	3.9	4.1	4.1	2.8	4.0	4.1
θ [-]	24	28	11	14	12	15	46	106
l_n [m]	0.67	0.60	0.72	0.55	0.38	2.6	2.1	3.2
l_a [m]	1.8	1.8	0.72	0.61	0.42	7.6	4.6	12
L [m]	2.0	1.9	2.2	2.2	1.3	1.0	4.4	3.5
$s(l_a)$ [(m^3/s)/m]	0.0088	0.013	0.0025	0.011	0.015			
$s(L)$ [(m^3/s)/m]						0.27	0.10	0.37
$c(l_a)$ [-]	0.37	0.47	0.14	0.43	0.60			
$c(L)$ [-]						0.60	0.50	0.60

Table A.3.1 Application of Mastbergen and Winterwerp (1987), with C as given in Table 4.1, to the Schelde Flume experiments T3 ($D_{50} = 0.10$ mm) and T5A ($D_{50} = 0.22$ mm) and the Zwin'89 experiment.

		Schelde Flume experiments						Zwin'89 exp.	
D_{50}	[mm]	0.10		0.22				0.22	
t	[s]	10	30	10	30	100	240	45	240
β	[°]	20	23	20	28	32	32	25	32
q_T	[(m^3/s)/m]	0.015	0.015	0.015	0.015	0.010	0.18	0.10	0.25
C	[-]	0.0125	0.0125	0.0125	0.0125	0.0125	0.0125	0.0125	0.0125
u	[m/s]	1.6	1.7	1.6	1.8	1.6	2.1	3.2	3.9
d	[m]	0.0094	0.0090	0.0094	0.0085	0.0062	0.086	0.031	0.065
θ	[-]	20	21	8.9	11	9.1	15	36	56
l_n	[m]	1.1	1.1	1.1	1.0	0.74	5.0	3.6	6.3
l_a	[m]	1.8	1.8	1.1 (0.57)	1.0 (0.61)	0.74 (0.42)	7.6	4.6	12
L	[m]	2.0	1.9	2.2	2.2	1.3	1.0	4.4	3.5
$s(l_a)$	[(m^3/s)/m]	0.0072	0.011	0.0028	0.015	0.015			
$s(L)$	[(m^3/s)/m]						0.27	0.084	0.37
$c(l_a)$	[-]	0.32	0.41	0.16	0.50	0.60			
$c(L)$	[-]						0.60	0.46	0.60

Table A.3.2 Application of Mastbergen and Winterwerp (1987), with $C = 0.0125$, to the Schelde Flume experiments T3 ($D_{50} = 0.10$ mm) and T5A ($D_{50} = 0.22$ mm) and the Zwin'89 experiment.

	Schelde Flume experiments						Zwin'89 exp.	
D_{50} [mm]	0.10		0.22				0.22	
t [s]	10	30	10	30	100	240	45	240
β [°]	20	23	20	28	32	32	25	32
q_T [(m^3/s)/m]	0.015	0.015	0.015	0.015	0.010	0.18	0.10	0.25
u [m/s]	1.3	1.3	1.3	1.3	1.2	2.4	2.5	3.5
d [m]	0.012	0.012	0.011	0.011	0.0085	0.074	0.040	0.072
$Re_\star$ [-]	18	19	39	45	42	46	60	90
θ_{cr} [-]	0.03	0.03	0.035	0.035	0.035	0.035	0.035	0.04
θ [-]	24	28	11	14	12	15	46	106
l_n [m]	0.67	0.60	0.72	0.55	0.38	2.6	2.1	3.2
l_a [m]	1.8	1.8	0.72	0.61	0.42	7.6	4.6	12
L [m]	2.0	1.9	2.2	2.2	1.3	1.0	4.4	3.5
$s_b(l_n)$ [(m^3/s)/m]	-	-	-	-	-		-	-
$s_b(L)$ [(m^3/s)/m]						-		
$c(l_n)$ or $c(L)$ [-]	-	-	-	-	-	-	-	-

Table A.4 Application of Mizuyama (1977) to the Schelde Flume experiments T3 ($D_{50} = 0.10$ mm) and T5A ($D_{50} = 0.22$ mm) and the Zwin'89 experiment.

		Schelde Flume experiments						Zwin'89 exp.	
D_{50}	[mm]	0.10		0.22				0.22	
t	[s]	10	30	10	30	100	240	45	240
β	[°]	20	23	20	28	32	32	25	32
q_T	[(m^3/s)/m]	0.015	0.015	0.015	0.015	0.010	0.18	0.10	0.25
C	[-]	0.025	0.027	0.022	0.028	0.032	0.0089	0.026	0.032
u	[m/s]	1.3	1.3	1.3	1.3	1.2	2.4	2.5	3.5
d	[m]	0.012	0.012	0.011	0.011	0.0085	0.074	0.040	0.072
$Re_\star$	[-]	18	19	39	45	42	46	60	90
$\theta_{cr}(\beta)$	[-]	0.01	0.01	0.01	0.005	0	0	0.005	0
Fr	[-]	3.7	3.8	3.9	4.1	4.1	2.8	4.0	4.1
θ	[-]	24	28	11	14	12	15	46	106
l_n	[m]	0.67	0.60	0.72	0.55	0.38	2.6	2.1	3.2
l_a	[m]	1.8	1.8	0.72	0.61	0.42	7.6	4.6	12
L	[m]	2.0	1.9	2.2	2.2	1.3	1.0	4.4	3.5
$s_b(l_n)$	[(m^3/s)/m]	0.0076	0.0095	0.0075	0.013	0.011		0.071	0.27
$s_b(L)$	[(m^3/s)/m]						0.026		
$c(l_n)$	[-]	0.34	0.39	0.33	0.46	0.52		0.42	0.52
$c(L)$	[-]						0.13		

Table A.5 Application of Smart en Jaeggi (1983) to the Schelde Flume experiments T3 ($D_{50} = 0.10$ mm) and T5A ($D_{50} = 0.22$ mm) and the Zwin'89 experiment.

		Schelde Flume experiments						Zwin'89 exp.	
D_{50}	[mm]	0.10		0.22				0.22	
t	[s]	10	30	10	30	100	240	45	240
β	[°]	20	23	20	28	32	32	25	32
q_T	[(m^3/s)/m]	0.015	0.015	0.015	0.015	0.010	0.18	0.10	0.25
$q_{cr} * 10^4$	[(m^3/s)/m]	0.013	0.011	0.041	0.027	0.023	0.023	0.031	0.023
u	[m/s]	1.3	1.3	1.3	1.3	1.2	2.4	2.5	3.5
d	[m]	0.012	0.012	0.011	0.011	0.0085	0.074	0.040	0.072
Fr	[-]	3.7	3.8	3.9	4.1	4.1	2.8	4.0	4.1
θ	[-]	24	28	11	14	12	15	46	106
l_n	[m]	0.67	0.60	0.72	0.55	0.38	2.6	2.1	3.2
l_a	[m]	1.8	1.8	0.72	0.61	0.42	7.6	4.6	12
L	[m]	2.0	1.9	2.2	2.2	1.3	1.0	4.4	3.5
$s_b(l_n)$	[(m^3/s)/m]	0.0031	0.0039	0.0031	0.0055	0.0047		0.030	0.12
$s_b(L)$	[(m^3/s)/m]						0.084		
$c(l_n)$	[-]	0.17	0.21	0.17	0.27	0.32		0.23	0.32
$c(L)$	[-]						0.32		

Table A.6 Application of Bathurst, Graf and Cao (1987) to the Schelde Flume experiments T3 ($D_{50} = 0.10$ mm) and T5A ($D_{50} = 0.22$ mm) and the Zwin'89 experiment.

		Schelde Flume experiments						Zwin'89 exp.	
D_{50}	[mm]	0.10		0.22				0.22	
t	[s]	10	30	10	30	100	240	45	240
β	[°]	20	23	20	28	32	32	25	32
q_T	[(m^3/s)/m]	0.015	0.015	0.015	0.015	0.010	0.18	0.10	0.25
C	[-]	0.16	0.23	0.16	0.41	0.68	0.65	0.28	0.65
u	[m/s]	0.68	0.63	0.68	0.55	0.42	1.1	1.1	1.3
d	[m]	0.022	0.024	0.022	0.027	0.024	0.16	0.088	0.20
Fr	[-]	1.5	1.3	1.5	1.1	0.88	0.90	1.2	0.91
θ	[-]	45	56	21	36	34	232	104	289
l_n	[m]	0.075	0.044	0.072	0.009	0	0	0.10	0
l_a	[m]	1.8	1.8	0.57	0.61	0.42	7.6	4.6	12
L	[m]	2.0	1.9	2.2	2.2	1.3	1.0	4.4	3.5
$s_b(l_n)$	[(m^3/s)/m]	0.0092	0.012	0.0094	0.018	0.015	0.27	0.096	0.37
$c(l_n)$	[-]	0.38	0.44	0.39	0.55	0.60	0.60	0.49	0.60

Table A.7 Application of Takahashi (1987) to the Schelde Flume experiments T3 ($D_{50} = 0.10$ mm) and T5A ($D_{50} = 0.22$ mm) and the Zwin'89 experiment.

		Schelde Flume experiments						Zwin'89 exp.	
D_{50}	[mm]	0.10		0.22				0.22	
t	[s]	10	30	10	30	100	240	45	240
β	[°]	20	23	20	28	32	32	25	32
q_T	[(m^3/s)/m]	0.015	0.015	0.015	0.015	0.010	0.18	0.10	0.25
$q_{cr} * 10^4$	[(m^3/s)/m]	0.015	0.012	0.048	0.031	0.026	0.026	0.036	0.026
u	[m/s]	1.3	1.3	1.3	1.3	1.2	2.4	2.5	3.5
d	[m]	0.012	0.012	0.011	0.011	0.0085	0.074	0.040	0.072
Fr	[-]	3.7	3.8	3.9	4.1	4.1	2.8	4.0	4.1
θ	[-]	24	28	11	14	12	15	46	106
l_n	[m]	0.67	0.60	0.72	0.55	0.38	2.6	2.1	3.2
l_a	[m]	1.8	1.8	0.72	0.61	0.42	7.6	4.6	12
L	[m]	2.0	1.9	2.2	2.2	1.3	1.0	4.4	3.5
$s_b(l_n)$	[(m^3/s)/m]	0.013	0.017	0.012	0.022	0.015		0.14	0.37
$s_b(L)$	[(m^3/s)/m]						0.27		
$c(l_n)$	[-]	0.46	0.53	0.45	0.60	0.60		0.57	0.60
$c(L)$	[-]						0.60		

Table A.8 Application of Rickenmann (1991) to the Schelde Flume experiments T3 ($D_{50} = 0.10$ mm) and T5A ($D_{50} = 0.22$ mm) and the Zwin'89 experiment.

		Schelde Flume experiments						Zwin'89 exp.	
D_{50}	[mm]	0.10		0.22				0.22	
t	[s]	10	30	10	30	100	240	45	240
β	[°]	20	23	20	28	32	32	25	32
C	[-]	0.025	0.027	0.022	0.028	0.032	0.0089	0.026	0.032
u	[m/s]	1.3	1.3	1.3	1.3	1.2	2.4	2.5	3.5
d	[m]	0.012	0.012	0.011	0.011	0.0085	0.074	0.040	0.072
Fr	[-]	3.7	3.8	3.9	4.1	4.1	2.8	4.0	4.1
$u_\star/w_s$	[-]	22	24	7.0	8.1	7.5	8.2	17	26
θ	[-]	24	28	11	14	12	15	46	106
l_n	[m]	0.67	0.60	0.72	0.55	0.38	2.6	2.1	3.2
l_a	[m]	1.8	1.8	0.72	0.61	0.42	7.6	4.6	12
L	[m]	2.0	1.9	2.2	2.2	1.3	1.0	4.4	3.5
$s_t(l_a)$	[(m^3/s)/m]	0.022	0.022	0.011	0.019	0.011			
$s_t(L)$	[(m^3/s)/m]						0.061	0.37	2.4
$s(L)$	[(m^3/s)/m]						0.0080	0.15	0.37
$c(l_a)$	[-]	0.60	0.60	0.43	0.55	0.52			
$c(L)$	[-]						0.042	0.60	0.60

Table A.9 Application of Engelund and Hansen (1967) to the Schelde Flume experiments T3 ($D_{50} = 0.10$ mm) and T5A ($D_{50} = 0.22$ mm) and the Zwin'89 experiment.

		Schelde Flume experiments						Zwin'89 exp.	
D_{50}	[mm]	0.10		0.22				0.22	
t	[s]	10	30	10	30	100	240	45	240
β	[°]	20	23	20	28	32	32	25	32
C	[-]	0.025	0.027	0.022	0.028	0.032	0.0089	0.026	0.032
u	[m/s]	1.3	1.3	1.3	1.3	1.2	2.4	2.5	3.5
d	[m]	0.012	0.012	0.011	0.011	0.0085	0.074	0.040	0.072
θ_{cr}	[-]	0.10	0.10	0.050	0.050	0.050	0.050	0.055	0.055
θ	[-]	24	28	11	14	12	15	46	106
l_n	[m]	0.67	0.60	0.72	0.55	0.38	2.6	2.1	3.2
l_a	[m]	1.8	1.8	0.72	0.61	0.42	7.6	4.6	12
L	[m]	2.0	1.9	2.2	2.2	1.3	1.0	4.4	3.5
$s_b * 10^3$	[(m^3/s)/m]	0.10	0.10	0.37	0.40	0.32	0.91	1.2	2.4
$s_s(l_a)$	[(m^3/s)/m]	0.0034	0.0036	0.0018	0.0021	0.0015			
$s_t(l_a)$	[(m^3/s)/m]	0.0035	0.0037	0.0022	0.0025	0.0019			
$s_s(L)$	[(m^3/s)/m]						0.0072	0.015	0.046
$s(L)$	[(m^3/s)/m]						0.0019	0.016	0.015
$c(l_a)$	[-]	0.19	0.20	0.13	0.14	0.16			
$c(L)$	[-]						0.010	0.14	0.058

Table A.10 Application of Van Rijn (1984a, 1984c) to the Schelde Flume experiments T3 ($D_{50} = 0.10$ mm) and T5A ($D_{50} = 0.22$ mm) and the Zwin'89 experiment.

		Schelde Flume experiments						Zwin'89 exp.	
D_{50}	[mm]	0.10		0.22				0.22	
t	[s]	10	30	10	30	100	240	45	240
β	[°]	20	23	20	28	32	32	25	32
C	[-]	0.025	0.027	0.022	0.028	0.032	0.0089	0.026	0.032
u	[m/s]	1.3	1.3	1.3	1.3	1.2	2.4	2.5	3.5
d	[m]	0.012	0.012	0.011	0.011	0.0085	0.074	0.040	0.072
Fr	[-]	3.7	3.8	3.9	4.1	4.1	2.8	4.0	4.1
θ	[-]	24	28	11	14	12	15	46	106
l_n	[m]	0.67	0.60	0.72	0.55	0.38	2.6	2.1	3.2
l_a	[m]	1.8	1.8	0.72	0.61	0.42	7.6	4.6	12
L	[m]	2.0	1.9	2.2	2.2	1.3	1.0	4.4	3.5
s_b	[(m^3/s)/m]	0.0016	0.0023	0.0016	0.0060	∞	∞	0.021	∞
$s_s(l_a)$	[(m^3/s)/m]	∞	∞	∞	∞	∞			
$s(l_a)$	[(m^3/s)/m]	0.022	0.022	0.022	0.022	0.015			
$s_s(L)$	[(m^3/s)/m]						∞	∞	∞
$s(L)$	[(m^3/s)/m]						0.27	0.15	0.37
$c(l_a)$	[-]	0.60	0.60	0.60	0.60	0.60			
$c(L)$	[-]						0.60	0.60	0.60

Table A.11 Application of Bagnold (1963, 1966) to the Schelde Flume experiments T3 ($D_{50} = 0.10$ mm) and T5A ($D_{50} = 0.22$ mm) and the Zwin'89 experiment.

		Schelde Flume experiments						Zwin'89 exp.	
D_{50}	[mm]	0.10		0.22				0.22	
t	[s]	10	30	10	30	100	240	45	240
β	[°]	20	23	20	28	32	32	25	32
q_T	[m²/s]	0.015	0.015	0.015	0.015	0.010	0.18	0.10	0.25
C	[-]	0.025	0.027	0.022	0.028	0.032	0.0089	0.026	0.032
u	[m/s]	1.3	1.3	1.3	1.3	1.2	2.4	2.5	3.5
d	[m]	0.012	0.012	0.011	0.011	0.0085	0.074	0.040	0.072
$u_\star/w_s$	[-]	22	24	7.0	8.1	7.5	8.2	17	26
θ	[-]	24	28	11	14	12	15	46	106
l_n	[m]	0.67	0.60	0.72	0.55	0.38	2.6	2.1	3.2
l_a	[m]	1.8	1.8	0.72	0.61	0.42	7.6	4.6	12
L	[m]	2.0	1.9	2.2	2.2	1.3	1.0	4.4	3.5
c_t	[-]	2.1	2.3	0.51	0.65	0.69	1.4	0.84	0.88
$s_t(l_a)$	[m²/s]	0.022	0.022	0.016	0.022	0.015			
$s_t(L)$	[m²/s]						0.27	0.15	0.37
$s(L)$	[m²/s]						0.27	0.15	0.37
$c(l_a)$	[-]	0.60	0.60	0.51	0.60	0.60			
$c(L)$	[-]						0.60	0.60	0.60

Table A.12 Application of Yang (1979) to the Schelde Flume experiments T3 ($D_{50} = 0.10$ mm) and T5A ($D_{50} = 0.22$ mm) and the Zwin'89 experiment.

		Schelde Flume experiments						Zwin'89 exp.	
D_{50}	[mm]	0.10		0.22				0.22	
t	[s]	10	30	10	30	100	240	45	240
β	[°]	20	23	20	28	32	32	25	32
C	[-]	0.025	0.027	0.022	0.028	0.032	0.0089	0.026	0.032
u	[m/s]	1.3	1.3	1.3	1.3	1.2	2.4	2.5	3.5
d	[m]	0.012	0.012	0.011	0.011	0.0085	0.074	0.040	0.072
Fr	[-]	3.7	3.8	3.9	4.1	4.1	2.8	4.0	4.1
$u_\star/w_s$	[-]	22	24	7.0	8.1	7.5	8.2	17	26
θ	[-]	24	28	11	14	12	15	46	106
l_n	[m]	0.67	0.60	0.72	0.55	0.38	2.6	2.1	3.2
l_a	[m]	1.8	1.8	0.72	0.61	0.42	7.6	4.6	12
L	[m]	2.0	1.9	2.2	2.2	1.3	1.0	4.4	3.5
s_b	[m^2/s]	$s_b << s_s$							
$s_s(l_a)$	[m^2/s]	0.0090	0.014	0.0018	0.0027	0.0018			
$s_s(L)$	[m^2/s]						0.015	0.052	1.1
$s(L)$	[m^2/s]						0.0019	0.050	0.31
$c(l_a)$	[-]	0.38	0.48	0.10	0.15	0.15			
$c(L)$	[-]						0.011	0.33	0.56

Table A.13 Application of Bagnold-Bailard (1981) to the Schelde Flume experiments T3 ($D_{50} = 0.10$ mm) and T5A ($D_{50} = 0.22$ mm) and the Zwin'89 experiment.

		Schelde Flume experiments						Zwin'89 exp.	
D_{50}	[mm]	0.10		0.22				0.22	
t	[s]	10	30	10	30	100	240	45	240
β	[°]	20	23	20	28	32	32	25	32
C	[-]	0.025	0.027	0.022	0.028	0.032	0.0089	0.026	0.032
u	[m/s]	1.3	1.3	1.3	1.3	1.2	2.4	2.5	3.5
d	[m]	0.012	0.012	0.011	0.011	0.0085	0.074	0.040	0.072
Fr	[-]	3.7	3.8	3.9	4.1	4.1	2.8	4.0	4.1
$u_\star/w_s$	[-]	22	24	7.0	8.1	7.5	8.2	17	26
θ	[-]	24	28	11	14	12	15	46	106
l_n	[m]	0.67	0.60	0.72	0.55	0.38	2.6	2.1	3.2
l_a	[m]	1.8	1.8	0.72	0.61	0.42	7.6	4.6	12
L	[m]	2.0	1.9	2.2	2.2	1.3	1.0	4.4	3.5
s_b	[m²/s]	$s_b << s_s$							
$s_s(l_a)$	[m²/s]	0.0050	0.0060	0.0017	0.0026	0.0019			
$s_s(L)$	[m²/s]						0.0094	0.032	0.16
$s(L)$	[m²/s]						0.0012	0.030	0.046
$c(l_a)$	[-]	0.25	0.28	0.099	0.15	0.16			
$c(L)$	[-]						0.0068	0.23	0.15

Table A.14 Application of Bagnold-Visser (1988) to the Schelde Flume experiments T3 ($D_{50} = 0.10$ mm) and T5A ($D_{50} = 0.22$ mm) and the Zwin'89 experiment.

		Schelde Flume experiments						Zwin'89 exp.	
D_{50}	[mm]	0.10		0.22				0.22	
t	[s]	10	30	10	30	100	240	45	240
β	[°]	20	23	20	28	32	32	25	32
C	[-]	0.025	0.027	0.022	0.028	0.032	0.0089	0.026	0.032
u	[m/s]	1.3	1.3	1.3	1.3	1.2	2.4	2.5	3.5
d	[m]	0.012	0.012	0.011	0.011	0.0085	0.074	0.040	0.072
Fr	[-]	3.7	3.8	3.9	4.1	4.1	2.8	4.0	4.1
u_*/w_s	[-]	22	24	7.0	8.1	7.5	8.2	17	26
θ	[-]	24	28	11	14	12	15	46	106
l_n	[m]	0.67	0.60	0.72	0.55	0.38	2.6	2.1	3.2
l_a	[m]	1.8	1.8	0.72	0.61	0.42	7.6	4.6	12
L	[m]	2.0	1.9	2.2	2.2	1.3	1.0	4.4	3.5
$s_t(l_a)$	[m^2/s]	0.022	0.022	0.022	0.022	0.015			
$s_t(L)$	[m^2/s]						∞	25	∞
$s(L)$	[m^2/s]						0.27	0.15	0.37
$c(l_a)$	[-]	0.60	0.60	0.60	0.60	0.60			
$c(L)$	[-]						0.60	0.60	0.60

Table A.15 Application of Takahashi (1991) to the Schelde Flume experiments T3 ($D_{50} = 0.10$ mm) and T5A ($D_{50} = 0.22$ mm) and the Zwin'89 experiment.

	Schelde Flume experiments						Zwin'89 exp.	
D_{50} [mm]	0.10		0.22				0.22	
t [s]	10	30	10	30	100	240	45	240
C [-]	0.025	0.027	0.022	0.028	0.032	0.0089	0.026	0.032
measured $s(l_n)$ [(m^3/s)/m]	0.0011	0.0020	0.0018	0.0019	0.0010		0.0057	0.047
measured $s(l_a)$ [(m^3/s)/m]	0.0040	0.0060	0.0018	0.0020	0.0012			
measured $s(L)$ [(m^3/s)/m]						0.0022	0.025	0.051
Wilson (1987)	0.0058	0.0069	0.0055	0.0085	0.0067	0.0087	0.049	0.17
Mastbergen and Winterwerp (1987)	0.0088	0.013	0.0025	0.011	0.015	0.27	0.10	0.37
Smart and Jaeggi (1983)	0.0076	0.0095	0.0075	0.013	0.011	0.026	0.071	0.27
Bathurst, Graf and Cao (1987)	0.0031	0.0039	0.0031	0.0055	0.0047	0.084	0.030	0.12
Takahashi (1987)	0.0092	0.012	0.0094	0.018	0.015	0.27	0.096	0.37
Rickenmann (1991)	0.013	0.017	0.012	0.022	0.015	0.27	0.14	0.37
Engelund and Hansen (1967)	0.022	0.022	0.011	0.019	0.011	0.0080	0.15	0.37
Van Rijn (1984a, 1984c)	0.0035	0.0037	0.0022	0.0025	0.0019	0.0019	0.016	0.015
Bagnold (1963, 1966)	0.022	0.022	0.022	0.022	0.015	0.27	0.15	0.37
Yang (1979)	0.022	0.022	0.016	0.022	0.015	0.27	0.15	0.37
Bagnold-Bailard (1981)	0.0090	0.014	0.0018	0.0027	0.0018	0.0019	0.050	0.31
Bagnold-Visser (1988)	0.0050	0.0060	0.0017	0.0026	0.0019	0.0012	0.030	0.046
Takahashi (1991)	0.022	0.022	0.022	0.022	0.015	0.27	0.15	0.37

Table A.16 Summary of experimental and computed sand transport rates (in (m^3/s)/m).

	Schelde Flume experiments						Zwin'89 exp.	
D_{50} [mm]	0.10		0.22				0.22	
t [s]	10	30	10	30	100	240	45	240
C [-]	0.025	0.027	0.022	0.028	0.032	0.0089	0.026	0.032
measured $s(l_n)$ [(m^3/s)/m]	0.0011	0.0020	0.0018	0.0019	0.0010		0.0057	0.047
measured $s(l_a)$ [(m^3/s)/m]	0.0040	0.0060	0.0018	0.0020	0.0012			
measured $s(L)$ [(m^3/s)/m]						0.0022	0.025	0.051
Wilson (1987)	5.3	3.4	3.1	4.5	6.7	4.0	8.6	3.6
Mastbergen and Winterwerp (1987)	2.2	2.2	1.4	5.5	12	123	4.0	7.3
Smart and Jaeggi (1983)	6.9	4.8	4.2	6.8	11	12	12	5.7
Bathurst, Graf and Cao (1987)	2.8	2.0	1.7	2.9	4.7	38	5.3	2.6
Takahashi (1987)	8.4	6.0	5.2	9.5	15	123	17	7.9
Rickenmann (1991)	12	8.5	6.7	12	15	123	25	7.9
Engelund and Hansen (1967)	5.5	3.7	6.1	9.5	9.2	3.6	6.0	7.3
Van Rijn (1984a, 1984c)	0.88	0.62	1.2	1.2	1.6	0.86	0.64	0.29
Bagnold-Bailard (1981)	2.2	2.3	1.0	1.3	1.5	0.86	2.0	6.1
Bagnold-Visser (1988)	1.2	1.0	0.94	1.3	1.6	0.55	1.2	0.90

Table A.17 Values of the ratio ζ between computed and experimental sand transport rates.

		Schelde Flume experiments						Zwin'89 exp.	
D_{50}	[mm]	0.10		0.22				0.22	
t	[s]	10	30	10	30	100	240	45	240
C	[-]	0.025	0.027	0.022	0.028	0.032	0.0089	0.026	0.032
measured $s(l_a)$	[(m^3/s)/m]	0.0040	0.0060	0.0018	0.0020	0.0012			
measured $s(L)$	[(m^3/s)/m]						0.0022	0.025	0.051
Wilson (1987)		1.4	1.2	3.1	4.2	5.6	0.53	1.9	0.97
Mastbergen and Winterwerp (1987)		2.2	2.2	1.4	5.5	12	123	4.0	7.3
Smart and Jaeggi (1983)		1.9	1.6	4.2	6.5	9.2	1.6	2.7	1.5
Bathurst, Graf en Cao (1987)		0.78	0.65	1.7	2.7	3.9	5.0	1.1	0.69
Takahashi (1987)		2.3	2.0	5.2	9.0	12	17	3.7	2.2
Rickenmann (1991)		3.2	2.8	6.7	11	12	26	5.4	3.3
Engelund and Hansen (1967)		5.5	3.7	6.1	9.5	9.2	3.6	6.0	7.3
Van Rijn (1984a, 1984c)		0.88	0.62	1.2	1.2	1.6	0.86	0.64	0.29
Bagnold-Bailard (1981)		2.2	2.3	1.0	1.3	1.5	0.86	2.0	6.1
Bagnold-Visser (1988)		1.2	1.0	0.94	1.3	1.6	0.55	1.2	0.90

Table A.18 Values of the ratio ζ between computed and experimental sand transport rates; sand transport rates computed assuming that sand transport has an adaptation length l_a, except for bed-load transport in Van Rijn's (1984a, 1984c) formulation.

	Schelde Flume experiments						Zwin'89 exp.	
D_{50} [mm]	0.10		0.22				0.22	
t [s]	10	30	10	30	100	240	45	240
C [-]	0.058	0.058	0.058	0.058	0.058	0.016	0.016	0.016
measured $s(l_a)$ [(m^3/s)/m]	0.0040	0.0060	0.0018	0.0020	0.0012			
measured $s(L)$ [(m^3/s)/m]						0.0022	0.025	0.051
Wilson (1987)	2.2	1.7	5.0	6.0	7.5	0.78	1.5	0.70
Mastbergen and Winterwerp (1987)	2.7	2.7	2.0	6.5	12	123	3.6	7.3
Smart and Jaeggi (1983)	2.0	1.6	4.2	6.5	8.3	1.7	2.7	1.6
Bathurst, Graf en Cao (1987)	0.78	0.65	1.7	2.7	3.9	5.0	1.1	0.69
Takahashi (1987)	2.3	2.0	5.2	9.0	12	17	3.7	2.2
Rickenmann (1991)	3.2	2.8	6.7	11	12	26	5.4	3.4
Engelund and Hansen (1967)	5.5	3.7	5.4	8.0	8.2	3.9	6.0	7.3
Van Rijn (1984a, 1984c)	0.48	0.40	0.67	1.0	1.2	0.77	0.68	0.36
Bagnold-Bailard (1981)	1.3	1.2	0.67	1.0	1.2	0.78	3.0	7.3
Bagnold-Visser (1988)	0.93	0.78	0.67	1.0	1.2	0.56	1.5	1.2

Table A.19 Values of the ratio ζ between computed and experimental sand transport rates; sediment transport rates computed with friction coefficient $C = 0.058$, or for the larger flow depths $C = 0.016$, and assuming that sand transport has an adaptation length l_a, except Van Rijn's (1984a, 1984c) bed-load transport.

	Schelde Flume experiments						Zwin'89 exp.	
D_{50} [mm]	0.10		0.22				0.22	
t [s]	10	30	10	30	100	240	45	240
C [-]	0.025	0.027	0.022	0.028	0.032	0.0089	0.026	0.032
l_a [m]	0.89	0.91	0.72	0.55	0.38	3.8	2.3	6.2
L [m]	2.0	1.9	2.2	2.2	1.3	1.0	4.4	3.5
measured $s(l_a)$ [$(m^3/s)/m$]	0.0015	0.0026	0.0018	0.0020	0.0011		0.010	
measured $s(L)$ [$(m^3/s)/m$]						0.0022		0.051
Wilson (1987)	3.9	2.7	3.1	4.2	6.1	1.0	4.9	1.9
Mastbergen and Winterwerp (1987)	2.8	2.5	1.4	5.0	14	123	5.2	7.3
Smart and Jaeggi (1983)	5.1	3.7	4.2	6.5	10	3.1	7.1	3.0
Bathurst, Graf and Cao (1987)	2.1	1.5	1.7	2.7	4.3	10	3.0	1.3
Takahashi (1987)	6.1	4.6	5.2	9.0	14	33	9.6	4.3
Rickenmann (1991)	8.7	6.5	6.7	11	14	52	14	6.7
Engelund and Hansen (1967)	15	8.6	6.1	9.5	10	7.3	15	7.3
Van Rijn (1984a, 1984c)	2.3	1.4	1.2	1.2	1.7	1.3	1.6	0.56
Bagnold-Bailard (1981)	6.0	5.4	1.0	1.3	1.6	1.8	5.2	7.3
Bagnold-Visser (1988)	3.3	2.3	0.94	1.3	1.7	1.1	3.2	1.8

Table A.20 Values of the ratio ζ between computed and experimental sand transport rates in case that sand transport has an adaptation length l_a, except Van Rijn's (1984a, 1984c) bed-load transport, and l_a is described by (4.4).

	Schelde Flume experiments						Zwin'89 exp.	
D_{50} [mm]	0.10		0.22				0.22	
t [s]	10	30	10	30	100	240	45	240
C [-]	0.025	0.027	0.022	0.028	0.032	0.0089	0.026	0.032
l_a [m]	3.5	3.6	1.1	1.2	0.84	15	9.2	25
L [m]	2.0	1.9	2.2	2.2	1.3	1.0	4.4	3.5
measured $s(l_a)$ [$(m^3/s)/m$]			0.0025	0.0036	0.0021			
measured $s(L)$ [$(m^3/s)/m$]	0.0046	0.0063				0.0022	0.025	0.051
Wilson (1987)	0.72	0.58	2.2	2.4	3.2	0.26	0.94	0.47
Mastbergen and Winterwerp (1987)	2.2	2.2	1.5	6.5	7.1	123	4.0	7.3
Smart and Jaeggi (1983)	0.94	0.80	3.0	3.6	5.2	0.79	1.4	0.74
Bathurst, Graf and Cao (1987)	0.39	0.33	1.2	1.5	2.2	2.5	0.57	0.33
Takahashi (1987)	1.1	1.0	3.8	5.0	7.1	8.5	1.8	1.1
Rickenmann (1991)	1.6	1.4	4.8	6.2	7.1	13.2	2.7	1.7
Engelund and Hansen (1967)	3.0	2.5	4.4	5.3	5.2	1.8	7.1	6.6
Van Rijn (1984a, 1984c)	0.43	0.31	0.88	0.69	0.90	0.63	0.33	0.17
Bagnold-Bailard (1981)	1.1	1.2	0.72	0.75	0.86	0.45	1.0	3.0
Bagnold-Visser (1988)	0.62	0.50	0.68	0.72	0.90	0.29	0.61	0.44

Table A.21 Values of the ratio ζ between computed and experimental sand transport rates in case that sand transport has an an adaptation length l_a, except Van Rijn's (1984a, 1984c) bed-load transport, and l_a is described by (4.5).

Appendix B List of main symbols

Symbol	Description	SI-unit
a	reference level in formulation of Van Rijn (1984c)	[m]
c	depth-averaged sand concentration (by volume)	[-]
c_a	sand concentration at height a above bottom	[-]
c_b	bed-load concentration	[-]
c_0	bed concentration	[-]
C	friction coefficient	[-]
d	water depth	[m]
d_n	normal flow depth (equilibrium value of water depth d)	[m]
d_c	critical flow depth	[m]
D	mean particle diameter	[m]
D_i	particle diameter such that i% of sediment volume has a diameter smaller than D_i	[m]
D_{50}	median particle diameter	[m]
Fr	Froude number $= u/\sqrt{gd}$	[-]
g	acceleration of gravity	[m/s^2]
H_d	height of dike (above polder surface)	[m]
H_w	water level against dike (above polder surface)	[m]
k	roughness factor	[m]
L	length inner slope	[m]
l_a	adaptation length of suspended load	[m]
l_n	length along inner slope over which the flow velocity approaches the normal flow velocity	[m]
p	bed porosity	[-]
q	flow discharge	[(m^3/s)/m]
q_T	flow discharge over dike top	[(m^3/s)/m]
r	ζ if $\zeta \geq 1$ and $1/\zeta$ if $\zeta < 1$	[-]
$\bar{r}$	mean value of r over eight cases under consideration	[-]
$Re_\star$	Reynolds number for flow around a sand particle $= u_\star D/\nu$	[-]
s_b, s_s, s_t	capacity of bed-load, suspended load and total load, respectively (subscript of s indicates a transport capacity)	[(m^3/s)/m]
$s(x)$	total transport at location x along the inner slope (s without subscript means the actual sediment transport, not necessarily the transport capacity)	[(m^3/s)/m]
t	time	[s]

List of main symbols (continuation)

Symbol	Description	SI-unit
u	depth-averaged flow velocity	[m/s]
u_n	normal flow velocity (equilibrium value of flow velocity u)	[m/s]
u_c	critical flow velocity	[m/s]
u_*	bed shear velocity	[m/s]
w_s	sediment fall velocity	[m/s]
x	coordinate along inner slope ($x = 0$ at the top of the inner slope)	[m]
z	coordinate normal to the inner slope ($z = 0$ at inner slope)	[m]
Z_T	height top of dike in breach (above polder surface)	[m]
β	inclination angle of inner slope	[°]
β_0	inclination angle of inner slope at t_0	[°]
β_1	critical value of β	[°]
Δ	specific density = $(\rho_s - \rho)/\rho$	[-]
θ	mobility parameter (Shields number)	[-]
θ_{cr}	critical value of θ for incipient motion	[-]
κ	constant of von Karman	[-]
μ	ripple factor (ratio of grain shear stress and total bed shear stress)	[-]
ν	kinematic viscosity	[m^2/s]
ζ	ratio (computed transport)/(measured transport)	[-]
ρ	water density	[kg/m^3]
ρ_s	sediment density	[kg/m^3]
τ_b	bed shear stress	[N/m^2]
ϕ	angle of repose of bed material	[°]